DESIGNING BOLT JOINTS OF FIXED-PITCH BUILT-UP SHIP PROPELLERS

Lappeenranta–Lahti University of Technology LUT

Master's Programme in Mechanical Engineering, Master's thesis

Master's programme in Industrial Design Engineering

2023

Ville Strömberg

Examiners: Professor Timo Björk

Timo Rauti, M.Sc. (Tech.)

ABSTRACT

Lappeenranta–Lahti University of Technology LUT

LUT School of Energy Systems

Mechanical Engineering

Ville Strömberg

Designing bolt joints of fixed-pitch built-up ship propellers

Master's thesis

2023

69 pages, 21 figures, 3 tables and 0 appendices

Examiners: Professor Timo Björk and Timo Rauti, M.Sc. (Tech.)

Keywords: bolt joints, built-up propellers, propeller blades

A method of designing bolt joints between the blades and hub of a fixed-pitch built-up ship propeller was studied in this thesis assigned by Steerprop Oy. Propeller design literature, classification rules and the VDI 2230 standard for calculating bolt joints were reviewed. A Microsoft Excel workbook was drawn up to calculate the bolt joints of a built-up propeller following the instructions of the standard. The distribution of loading among the bolts is calculated utilizing the rigid body method in the calculation tool. The tool was tested with input from an existing exemplary built-up propeller design, and the calculation results were compared with values extracted from a finite element calculation model. The studied propeller design has a curved bolt joint interface, and its properties were further studied by the finite element model and compared to a modified configuration with a planar interface.

The result of this work serves as a basis for further research, which is necessary before the Excel tool can be applied in practice. Notable differences were found between the outcome of finite element analysis and calculations of the newly developed workbook, mainly rising from the method of assessing bolt load distribution for which the rigid body method as such proved to be insufficient in this case. Loads assigned to each bolt affect the results of single-bolt joint calculations. To develop the calculation tool, modifying the rigid body model to calculate the required minimum clamp load by the criteria of preventing one-sided opening of the joint instead of the current application where friction is definitive could be studied, or a more complex elastomechanical approach could be considered. On the other hand, the Excel tool developed can also easily be converted to calculate simpler and more common bolt joints with planar interfaces and thus aid in their design.

TIIVISTELMÄ

Lappeenrannan–Lahden teknillinen yliopisto LUT

LUTin energiajärjestelmien tiedekunta

Konetekniikka

Ville Strömberg

Kiinteälapaisten laivan irtolapapotkureiden pulttiliitosten suunnittelu

Konetekniikan diplomityö

2023

69 sivua, 21 kuvaa, 3 taulukkoa ja 0 liitettä

Tarkastajat: Professori Timo Björk ja DI Timo Rauti

Avainsanat: irtolapapotkurit, potkurinlavat, pulttiliitokset

Tässä Steerprop Oy:n toimeksi antamassa diplomityössä tutkittiin metodia kiinteälapaisen laivan irtolapapotkurin lavan ja navan välisten pulttiliitosten suunnittelemiseksi. Tutustuttiin potkurisuunnittelua käsittelevään kirjallisuuteen, luokitussääntöihin ja pulttiliitosten laskennassa opastavaan VDI 2230 -standardiin. Pulttiliitosten laskemiseksi standardin ohjeita seuraten laadittiin Microsoft Excel -työkirja. Kuorman jakautuminen pulttien kesken lasketaan laskentatyökalussa jäykän kappaleen menetelmällä. Työkalua testattiin antamalla syötteeksi olemassa olevan esimerkkipotkurin mallin tietoja, ja laskennan tuloksia verrattiin arvoihin, jotka saatiin elementtimenetelmällä laskentamallista. Tutkitussa potkurimallissa pulttiliitospinta on kaareva, ja sen ominaisuuksia tutkittiin lisää elementtimenetelmällä ja verrattiin muokattuun malliin, jossa liitospinta on tasomainen.

Tämän työn tulos toimii pohjana lisätutkimuksille, jotka ovat välttämättömiä ennen kuin Excel-työkalua voi soveltaa käytännössä. Elementtimenetelmän analyysin ja kehitetyn uuden työkirjan tulosten välillä havaittiin huomattavia eroja. Erot johtuvat pääasiassa tavasta, jolla kuormat jaetaan pulttien kesken. Tähän tarkoitukseen jäykän kappaleen malli sellaisenaan osoittautui tässä tapauksessa riittämättömäksi. Kullekin pultille osoitetut kuormat vaikuttavat yksittäisten pulttiliitosten laskennan tuloksiin. Laskentatyökalun kehittämiseksi voisi tutkia jäykän kappaleen mallin muokkaamista siten, että tarvittava pienin puristuskuorma laskettaisiin yksipuolisen aukeamisen estämisen ehdoilla eikä nyt toteutetulla tavalla, jossa kitka on määräävä tekijä. Monimutkaisempaa elastomekaanista lähestymistapaakin voisi selvittää. Toisaalta laadittu Excel-työkalu on myös helppo muokata laskemaan yksinkertaisempia ja yleisempiä pulttiliitoksia, joilla on tasomainen liitospinta, ja näin auttamaan niiden suunnittelussa.

ACKNOWLEDGEMENTS

I am thankful to Professor Timo Björk and Antti Ahola, D.Sc. (Tech.), for their guidance and support during this thesis work.

I also wish to thank Steerprop Oy for providing me with an interesting and challenging topic. Special thanks to Timo Rauti and Tero Tamminen for their help and advice.

Finally, thanks to my family for all the patience during these action-packed times.

Ville Strömberg

Ville Strömberg

SYMBOLS AND ABBREVIATIONS

Roman characters

B	developed area ratio in propeller design	
b	width of expanded blade section at design root section	m
c	true chord length of propeller blade section	m
D	propeller diameter	m
D_b	bolt diameter or internal diameter of bolt thread (lesser one)	mm
D_C	bolt pitch circle diameter (in BV rules)	mm
d	bolt pitch circle diameter (in RMRS rules)	m
d_{PR}	diameter at the bottom of bolt thread	mm
$F_{A\,(M)}$	axial bolt load arising from the effect of moments	kN
F_{ex}	propeller blade failure load	kN
F_{qmax}	maximum transverse force	kN
F_y	force in the direction of the y-axis	kN
f	tabular material constant	
h_1	coefficient	mm
k	material correction factor (in ABS rules) coefficient (in RMRS rules)	
$l_{0.35}$	expanded width of propeller blade section at $0.35R$	mm
M_x	moment about x-axis	kNm
M_y	moment about y-axis	kNm
M_z	moment about z-axis	kNm
M_T	continuous transmitted torque	kNm

N	rotational speed of propeller	rpm
n	bolt count on the driving side of propeller blade	
n_{PR}	bolt count per propeller blade	
n_S	number of bolts in bolt array	
R	propeller radius	m
R_{mb}	tensile strength of bolt material (in RMRS rules)	MPa
R_{mbl}	tensile strength of blade material	MPa
$R_{m,PR}$	minimum tensile strength of bolt material (in BV rules)	N/mm^2
r	pitch circle radius (in ABS rules)	mm
	root section radius at the weakest point (in IACS rules)	m
r_{min}	radius between bolt array centroid and the bolt closest to it	mm
s	bolt area at thread bottom (in ABS rules)	mm^2
	maximum blade thickness at design root section (in RMRS rules)	mm
t	root section thickness at the weakest location outside root fillet	m
$t_{0.35}$	required minimum thickness of blade section at 0.35R	mm
W	expanded width of a controllable-pitch blade section at 0.35R	mm
z	propeller blade count	

Greek characters

α_i	angle between bolt axis and the vertical yz-plane	°
α_{xz}	angle between operating force and the horizontal xz-plane	°
α_y	angle between operating force and the vertical yz-plane	°
δ	blade material density	kg/dm^3
$\rho_{0.7}$	coefficient	

σ_{ref}	reference stress	MPa

Abbreviations

3D	Three-dimensional
ABS	American Bureau of Shipping
BV	Bureau Veritas
CP	Controllable-pitch
DNV	Det Norske Veritas
FE	Finite element
FEA	Finite element analysis
FEM	Finite element method
FSICR	Finnish-Swedish ice class rules
IACS	International Association of Classification Societies
ISO	International Organization for Standardization
LR	Lloyd's Register
NACA	National Advisory Committee for Aeronautics
NASA	National Aeronautics and Space Administration
RMRS	Russian Maritime Register of Shipping
VDI	Verein Deutscher Ingenieure, Association of German Engineers

Table of contents

Figures

Tables

1 Introduction

The object of this work is to research requirements placed on the bolt joints of blades of fixed-pitch built-up ship propellers, and applicable design processes and methods to meet those requirements. This thesis was assigned by Steerprop Oy, a Rauma-based company designing and providing azimuth propulsors for ships. A built-up propeller is a propeller whose blades are separate from the propeller hub and installed in place with bolts. Propellers of the type with controllable pitch by means of turning blades are also built-up, but this work is distinct from those and focused on propellers with fixed pitch. The study is motivated by the fact that, on the subcontracting market, specialized design know-how onto which the company has leaned is decreasing, while built-up propellers continue to be an important solution in the company's product portfolio. This is especially the case with icebreaker propulsion. Built-up propellers can provide economic and technical advantages in some cases through easier maintenance compared to monobloc propellers. It is crucially important for the safe and fault-free operation of a propulsor that the propeller and its possible bolt joints are properly dimensioned and that for example, in case of collision, propeller blades break before gears to keep damages to a minimum (DNV 2021b, 24). Ship propellers are typically tailored and optimized for individual ship hulls to ensure the best possible hydrodynamical and cost-efficiency, which is contrary to often mass-produced boat propellers (Bertram 2012, 43). Complex calculations are involved and no general solution fitting every need is possible. Propellers are geometrically complicated pieces.

Propeller design in general is covered in shipbuilding literature, such as works of Bertram (2012), Birk (2019), Carlton (2012) and Tupper (2013). However, there is little public research available on built-up propellers and connecting detachable propeller blades to the hub and hence there is a need for this study.

The research problem of this thesis is: how to design the bolt joints of a fixed-pitch built-up ship propeller? The information not being readily publicly available, this work aims to gather a list of necessary design information, requirements and available methods. This work aims to serve as a basis onto which a company's own design process can be defined. The thesis should also result in a way of roughly estimating whether a set of proposed bolts is adequate or to be rejected. Steerprop suggested studying the suitability of the German VDI 2230

standard for the task. To provide the company a tool for the calculations, a Microsoft Excel workbook is drawn up.

The research questions of this thesis are:

- How must the connection between propeller blades and hub be designed?
- What requirements have major classification societies set for bolt joints of built-up propellers?
- What design methods and processes are there available for use in the maritime industry for designing built-up propellers and especially their bolt joints? Is the VDI 2230 standard applicable?

Relevant rules of classification societies are reviewed in this thesis. Emphasis of this work is in designing bolted connections, and propeller geometry is mainly presumed given. However, the bolt joints and blade root geometry of a built-up propeller limit each other, and this interaction is discussed. Similarly, defining the magnitude and direction of the loading that acts on the propeller blade and whose effects are distributed among blade bolts falls outside the scope of this thesis and the load is taken as a given input. Results given by the new Excel workbook are compared to values extracted from a finite element (FE) model with similar input, and the validity and applicability of the tool are discussed.

2 Built-up propellers

Built-up propellers are propellers whose blades are separate pieces from the propeller hub or boss, contrarily in comparison with monobloc propellers more common today. Monobloc propellers are made as one piece, and built-up propeller blades are connected to a hub piece by bolts. The separate hub is an additional part that a monobloc propeller does not have. The hub is shrink-fitted onto propeller shaft in the same way as the boss of a monobloc propeller.

The portion of a built-up propeller blade root where bolt holes are located is called the blade's palm. An example of loose blades of a built-up propeller with fixed pitch is shown in Figure 1. Once installed in place, the blades in the figure cannot be rotated around any spindle axis (an axis roughly perpendicular to the blade palm), unlike in a controllable-pitch (CP) propeller whose operation is illustrated in Figure 2 to clarify the distinction. Bolt holes for fastening the fixed-pitch blades to the hub are well visible in Figure 1.

Figure 1. Blades of a fixed-pitch built-up propeller (Fincantieri n.d.).

A propeller's pitch either is fixed or can be altered by controlling blade angle around an axis normal to the propeller shaft, hence the name controllable-pitch propeller. Controllable pitch is different from variable pitch, in which blades have a pitch varying with radius and the blades are fixed as in Figure 1 (Birk 2019, 427; Tupper 2013, 192). Controllable pitch enables adjusting of thrust and reversing the ship with the main engine running at a constant speed and not needing a reverse gear as illustrated in Figure 2, but the hub necessarily is rather large and fuel consumption somewhat higher than that of a fixed-pitch propeller (Bertram 2012, 68–69). Built-up propellers generally are mechanically more complicated and more expensive to manufacture than monobloc propellers, and the pitch control ability further adds the complexity.

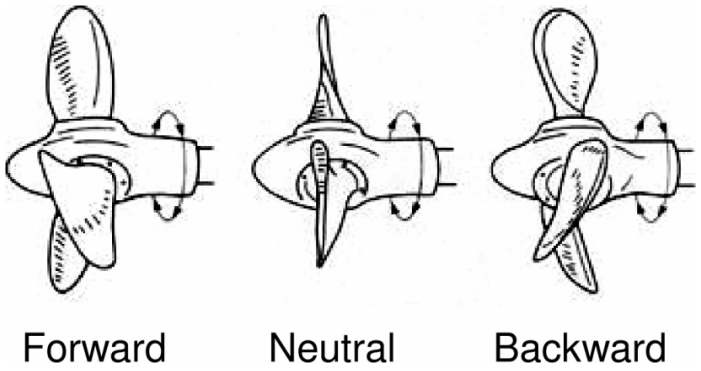

Figure 2. Controllable-pitch propeller and its operation modes (Doi, Nagamoto & Takehira 2013, 3000).

Figure 3 presents the proper names of propeller parts. Understanding the terminology is necessary when reading the rules of classification societies or describing propeller geometry. Some of the terms are rather specific and quite possibly unfamiliar to those not readily acquainted with propellers, so an introduction is in order. This work concerns itself with screw propellers, which are the most common means of propulsion in ships (Bertram 2012, 41; Birk 2019, 391). A screw propeller can be thought of as a portion of a helicoidal surface screwing its way forward underwater, though modern propellers in reality do not consist of a single helicoidal surface but rather several, with blade pitch varying with radius from the shaft axis (Bertram 2012, 42; Tupper 2013, 165–166). In Figure 3, there is a screw propeller with four blades seen from the aft side on the left and from ahead on the right side. The

shown propeller has a fixed pitch meaning the blades cannot rotate around axes roughly perpendicular to the shaft line. The central piece to which the blades are connected is called hub or boss. The interconnection between the hub and a blade is called the blade's root. A blade's edge farthest away from the hub is the blade's tip. The edge traveling ahead in the front while the propeller is rotating is called the leading edge. The edge following behind is the trailing edge. Blade surfaces on the aft side of the ship are blade faces and those on the fore side of the ship are blade backs. Blade face is the pressure side of the blade, and back is the suction side with low pressure (Birk 2019, 421).

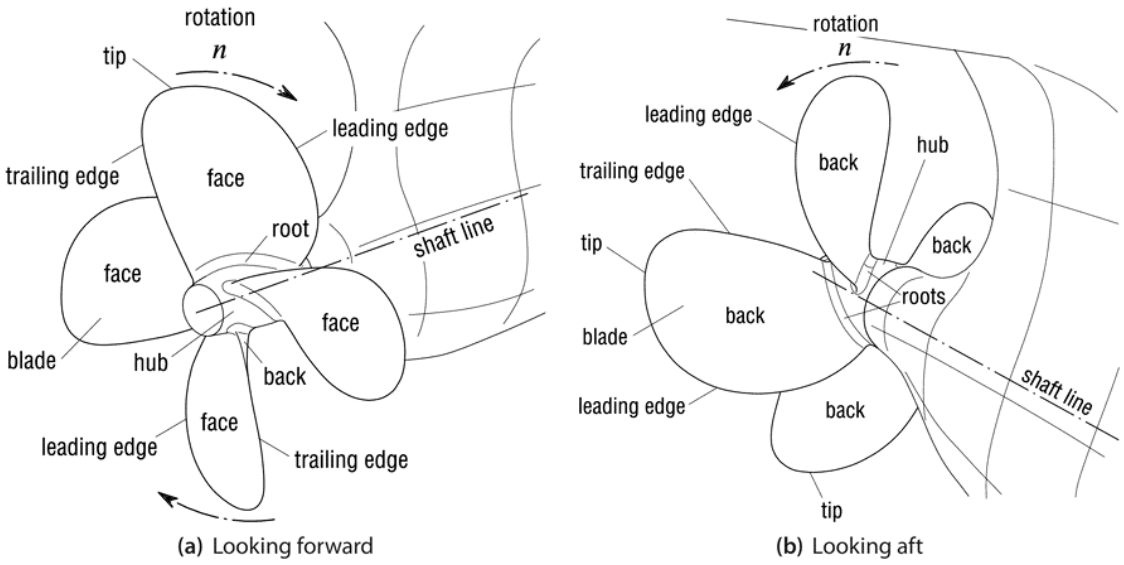

Figure 3. Parts of a right-handed, fixed-pitch propeller with four blades (Birk 2019, 421).

Propellers rotating clockwise, seen from aft, while producing thrust to move a ship forward, are said to be right-handed and similarly propellers rotating counterclockwise seen from aft are called left-handed (Bertram 2012, 41; Birk 2019, 421; Carlton 2012, 46; Tupper 2013, 168). Propellers must be dynamically balanced and hence the blades are always regularly arranged (Birk 2019, 421). Ship propellers typically have four to seven blades (Bertram 2012, 43; Birk 2019, 422; Carlton 2012, 12). Resonant frequencies harmful to ship structures and machinery are avoided by proper selection of the blade number (Bertram 2012, 231; Birk 2019, 422; Carlton 2012, 448). A higher blade number helps in avoiding vibration problems but makes the manufacturing of the propeller more expensive (Bertram 2012, 43)

and can cause cavitation problems at blade roots because less clearance is left between the blades (Carlton 2012, 448).

As Tupper (2013, 167) says, the sections of modern propeller blades are aerofoil (i.e., hydrofoil) shape, resembling sections of airplane wings. Propeller blade sections are not planar but intersections of the blade and a right circular cylinder whose axis is coincident with the propeller shaft line. Figure 4 illustrates the definition of a propeller blade section. The cylindrical sections are usually presented flattened. According to Carlton (2012, 38), certain aerofoils developed in the National Advisory Committee for Aeronautics (NACA; the predecessor of NASA, National Aeronautics and Space Administration) in the USA have been widely adopted for marine propeller design. However, NACA profiles are not the only aerofoils existing and in use.

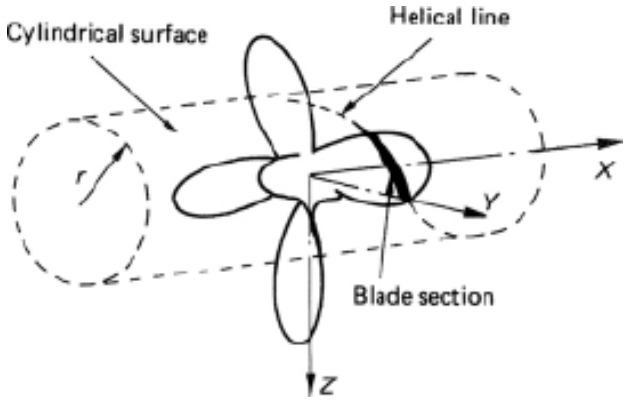

Figure 4. Propeller blade section (Carlton 2012, 30).

The primary propeller manufacturing method is casting. The most common propeller materials are bronzes, high-tensile brasses and stainless steels, although other materials such as duralumin, polymers and carbon fiber composites are used as well. Propeller material should have resistance against corrosion fatigue in seawater, cavitation erosion, general corrosion, and impingement attack and crevice corrosion. The combination of low weight and high strength is also preferrable. Considering manufacturing and repair operations, good weldability and castability are desirable. (Carlton 2012, 385–386.)

Built-up propellers are more complex to design than monobloc propellers. However, built-up propellers enable:

- propeller maintenance without dry-docking
- replacing only damaged blades and not the whole propeller
- easier handling (e.g., lifting) of spare blades compared to a monobloc propeller
- storing spare blades more easily due to a smaller space requirement, for example aboard the ship.

Considering manufacturing, built-up propellers are cast in smaller molds than monobloc ones but have more area that requires precise machining.

Blades of CP propellers are fastened with bolts, and thus, they are built-up, but built-up propellers are not necessarily of the CP type. McGeorge (1998, 272) recognizes the ability of adjusting propeller pitch and easy replacement of damaged propeller blades as benefits of built-up propellers but says that they also have limited blade root width, greater blade thickness and bigger hub diameter which lead to a decreased efficiency. Carlton (2012, 11) identifies blade root cavitation as a potential problem caused by a big hub. In the case of CP propellers, not only do the fastening bolts of the blade require some space in the propeller hub but the pitch control mechanism, too. Pitch control ability adds further design constraints for the built-up propeller compared to a fixed-pitch counterpart, for when changing the pitch, the blades must have room to rotate around their spindle axes without colliding with each other. Their fastening bolts also move along circular paths that cannot overlap.

The environment of the bolt joints at the root of built-up blades is limited in space, and the bolt holes and blade root geometry restrict each other. The area in question is visualized in Figure 5.

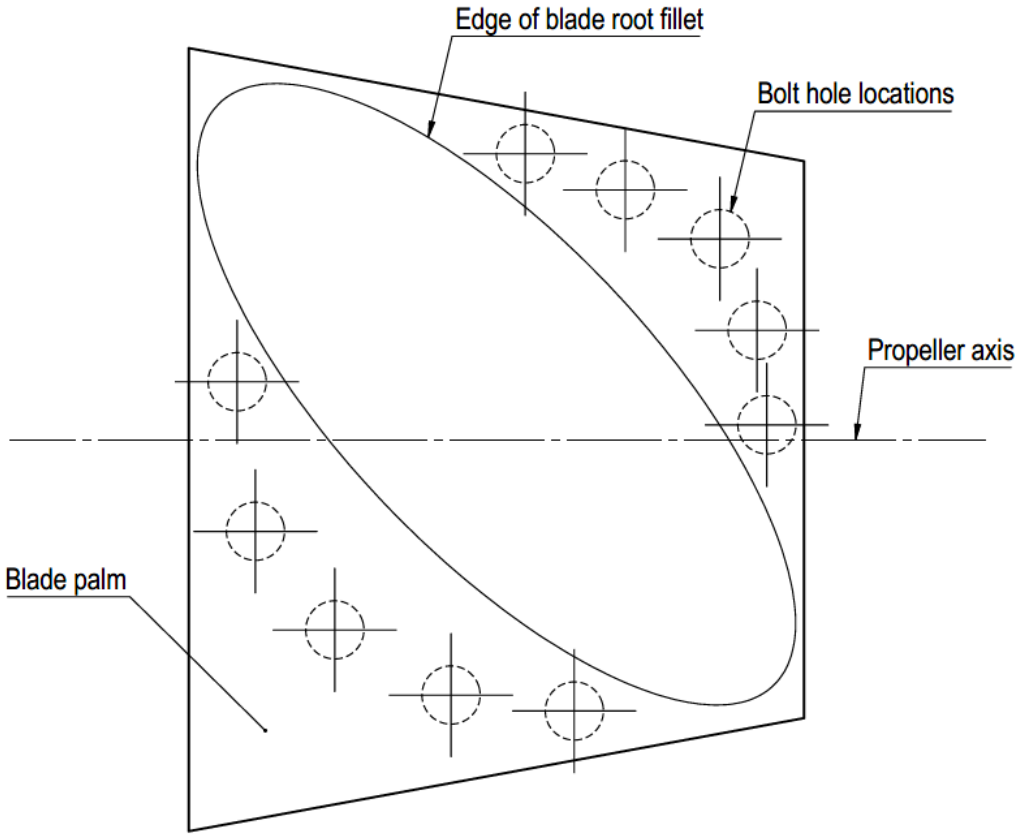

Figure 5. Sketch of built-up propeller blade root and palm area.

In the case of fixed-pitch propellers, the outer surfaces of blade palms are commonly simple sectors of the conical boss with an angle of a full circle divided by propeller blade count. The blade root and its root fillet must fit within the palm sector. Similarly, the bolt holes are to be located on the palm. A minimum distance to be kept from palm edges and between the bolts can be defined. Additionally, bolt holes must not overlap with critical areas of the root fillet. Considerations and adjustments to be made in this area during propeller design concern blade root width and position, root fillet geometry and the size, count and pattern of bolts and bolt holes. It is possible, for example, that the position of blade root needs to be moved or rotated slightly to make room for bolt holes, or, conversely, that in designing the bolt connection the bolt holes need to be relocated because modification of blade root is impossible due to design constraints.

3 Classification rules of built-up propellers

Classification rules concerning built-up propellers are reviewed in this chapter. The applicable main design principle is introduced first. Propeller blade root geometry and the palm area are touched upon secondly, and lastly, rules regarding the fasteners themselves are studied.

3.1 Pyramid strength principle

The design principle to be followed in making ice-classed propellers is the pyramid strength principle, also called selective strength principle. This design principle is included in the unified requirements of the International Association of Classification Societies (2007, 9), shortened IACS, and the Finnish-Swedish ice class rules, abbreviated FSICR (Finnish Transport and Communications Agency Traficom 2021, 47). As a unified requirement of IACS, this demand is made by all of its member societies, such as American Bureau of Shipping (ABS), Bureau Veritas (BV), DNV (originally Det Norske Veritas) and Lloyd's Register (LR). The main idea of the pyramid strength principle is that propeller blades must be the weakest part of the propulsion line and the loss or plastic bending of a blade must not damage any relevant successive parts such as propeller hub or shaft, thrust bearing, or thruster structures and supports. Ergo, the rest of the propulsion line must withstand the blade failure load, bolts of a built-up propeller blade being the next components in line. Figure 6 illustrates the pyramid strength principle. (American Bureau of Shipping 2022b, 66; Bureau Veritas 2021, 31; DNV 2021b, 24; Lloyd's Register 2021, 1800.)

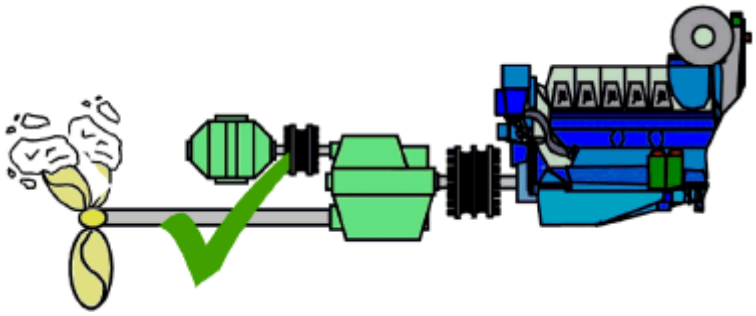

Figure 6. Pyramid strength principle (DNV 2021b, 24, modified).

Another important design principle implied by the four classification societies is that the propulsion line must be able to take maximum and fatigue operational loads under dynamic excitation plus a defined safety margin (American Bureau of Shipping 2022b, 66; Bureau Veritas 2021, 31; DNV 2021b, 33; Lloyd's Register 2021, 1800).

It follows from the pyramid strength principle that the bolt joints of a built-up propeller with an ice class must be dimensioned according to the blade failure load, which is the greatest load that the bolts must endure. The force causing the blade to fail is to be considered to act at 0.8R radius in the weakest direction of the blade, R being the propeller radius. The following equation presents the IACS formula for blade failure load, also written in the FSICR and rulebooks of ABS, BV, DNV and LR (American Bureau of Shipping 2022b, 65; Bureau Veritas 2021, 36; DNV 2022, 186; Finnish Transport and Communications Agency Traficom 2021, 45–46; Lloyd's Register 2021, 1799–1800):

$$F_{ex} = \frac{0.3ct^2\sigma_{ref}}{0.8D - 2r} \cdot 10^3 \quad (1)$$

where

- F_{ex} is the blade failure load [kN]
- c is the true chord length [m]
- t is the cylindrical root section thickness at the weakest location outside root fillet [m]

- σ_{ref} is reference stress [MPa]
- D is the propeller diameter [m]
- r is the cylindrical root section radius at the weakest location outside root fillet [m].

DNV and the FSICR consider a propeller blade lost due to plastic bending when the blade tip has bent a distance greater than 10% of the propeller diameter (DNV 2021b, 9; DNV 2022, 70; Finnish Transport and Communications Agency Traficom 2021, 45). The FSICR optionally allow the calculation of the blade failure load with the help of an elastoplastic FE model (Finnish Transport and Communications Agency Traficom & Swedish Transport Agency 2019, 29). The blade failure load calculated by either finite element method (FEM) or previously shown Equation 1 is input for the subsequent calculation of propeller bolt joints.

Ice class conditions must be met if a ship is meant to go through icy waters. Ice classing rules make difference between first year and multi-year ice, ice ridge thicknesses and ice conditions in which a ship should be able to make its way unassisted. The part of the world where the vessel is to navigate must naturally be considered. Ice class factors listed in the rules comprise design ice thickness and ice strength indexes for estimating propeller ice loads for each ice class. Ice classing adds requirements for propeller materials and geometry including blade width, thickness, edges and bolts. A great part of propeller ice class rules consists of the design loads according to which the propeller is dimensioned.

No specific load cases are named determinative in designing the bolt joints of propeller blades without an ice class. Thus, open water propellers are to be designed to withstand the worst combinations of all allowed circumstances. For blade bolts, this means that they must not yield in any allowed operating conditions (DNV 2021c, 16). However, open water propellers too can hit ground or rock, in which case following the pyramid strength principle voluntarily would limit and minimize the damage.

3.2 Propeller geometry

Classification societies regulate minimum fillet radii at blade roots. As DNV explains in its propeller design guideline, the purpose of the root fillet is to avoid excess stresses there, for which DNV and BV deem adequate a constant radius equal to or greater than 75% of the

required blade section thickness in that position (Bureau Veritas 2022, 184; DNV 2021a, 22). LR demands, at minimum, a fillet radius equal to the required section thickness (Lloyd's Register 2021, 1105), and Russian Maritime Register of Shipping (RMRS) defines the minimum fillet radius as 4% of propeller diameter on the suction side of a raked propeller and 3% of propeller diameter otherwise (Russian Maritime Register of Shipping 2022, 56). According to DNV guideline, stresses between recessed bolt holes in built-up blade flanges are to be treated similarly with blade root fillets (DNV 2021a, 22).

A single constant radius at blade root causes a stress concentration (Carlton 2012, 408). BV, DNV and LR also accept fillets with a varying radius providing constant stress and greater effective radius. ABS merely notes that blade root fillets are to be neglected in considering blade thicknesses (American Bureau of Shipping 2022a, 337). A similar remark is made by BV, LR and RMRS.

Material is the only aspect of the propeller hub addressed in classification rules. According to Carlton (2012, 449–450), the hub is best kept as small as possible. Subsequently, it is only dimensioned as large as blade strength and fasteners require. Hub form also has hydrodynamical importance and an effect on cavitation.

3.3 Propeller blade fasteners

Classification rules concerning the fasteners of built-up propeller blades are reviewed in this section. Calculation formulae for defining the required minimum bolt diameter are shown to point out what kinds of factors classification societies have recognized in the matter.

ABS notes that the fasteners of built-up blades must be fitted in place without reducing blade section area for making space and has further requirements for the blade flange and bolts of CP propellers (American Bureau of Shipping 2022a, 337), which could be applied to built-up fixed-pitch propellers, though this is not explicitly implied compulsory. The following equation gives the section area of a CP propeller blade bolt as required by ABS at the bottom of thread:

$$s = \frac{0.056 W k f t_{0.35}^2}{r n} \tag{2}$$

where

- s is bolt area at thread bottom [mm^2]
- W is expanded width of a cylindrical section of CP propeller blade at 0.35R (section radius 0.35 times the propeller radius R) [mm]
- k is material correction factor [–]
- f is tabular material constant [–]
- $t_{0.35}$ is the required minimum thickness at the thickest part of blade section at 0.35R [mm]
- r is pitch circle radius [mm]
- n is bolt count on the driving side of propeller blade [–].

LR necessitates the consideration of stress distribution in the built-up propeller's blade flange or palm (Lloyd's Register 2021, 1106). BV, DNV and RMRS have more specific rules concerning the bolt connections of built-up blades. In their rules, built-up blades are specifically named and not just CP propellers. BV and RMRS provide their own calculation formulae for the minimum bolt diameter. The BV formula is given in the equation below (Bureau Veritas 2022, 184):

$$d_{\mathrm{PR}} = \left(\frac{4.6\rho_{0.7} M_{\mathrm{T}} \cdot 10^7 + 0.88\delta \cdot \left(\frac{D}{10}\right)^3 \cdot B l_{0.35} N^2 h_1}{n_{\mathrm{PR}} z D_{\mathrm{C}} R_{\mathrm{m,PR}}} \right)^{0.5} \tag{3}$$

where:

- d_{PR} is the diameter at the bottom of bolt thread [mm]
- $\rho_{0.7}$ is a coefficient calculated by dividing propeller diameter by pitch at 0.7 radius from propeller axis [–]
- M_{T} is continuous transmitted torque [kNm]

- δ is blade material density [kg/dm^3]
- D is propeller diameter [m]
- B is developed area ratio of the propeller design [–]
- $l_{0.35}$ is the expanded width of blade section at 0.35R [mm]
- N is rotational speed of the propeller [rpm]
- h_1 is a factor equal to the sum of rake and 1.125 D_C [mm]
- n_{PR} is bolt count per blade [–]
- z is blade count [–]
- D_C is bolt pitch circle diameter [mm]
- $R_{m,PR}$ is the minimum tensile strength of bolt material [N/mm^2].

The RMRS equation for the same purpose is the following (Russian Maritime Register of Shipping 2022, 56):

$$D_b = ks\sqrt{\frac{bR_{mbl}}{dR_{mb}}} \tag{4}$$

where

- D_b is the lesser one out of bolt diameter and the internal diameter of bolt thread [mm]
- k is a coefficient dependent of bolt count in blade flange at thrust surface [–]
- s is maximum blade thickness at design root section [mm]
- b is the width of expanded cylindrical blade section at design root section [m]
- R_{mbl} is the tensile strength of blade material [MPa]
- d is bolt pitch circle diameter [m]
- R_{mb} is the tensile strength of bolt material [MPa].

For the factor *k* in the RMRS formula, value 0.33 is given for a count of three bolts, 0.30 for four bolts and 0.28 for five bolts, respectively. For other than circular bolt arrangements, the variable *d* equals 0.85 times the distance between the most distant bolts.

DNV (2021c, 16) has straightforward requirements for installing propeller blades with bolts. For built-up propellers without a pitch control mechanism, the general (non-ice class) rules regulate bolt pre-tension and safety factor for the high cycle stress of blade bolts. Bolt pre-tension stress must be the lesser one of the following:

- 50%–70% of bolt material yield strength
- maximum 56% of bolt tensile strength.

BV requires the blade bolts to be tightened to a pre-tension of approximately 60%–70% of yield strength (Bureau Veritas 2022, 184). The rules further dictate that the prestress must be maintained in all operating conditions for which the propeller is designed, and no allowed operating conditions may cause yielding of bolt material (DNV 2021c, 16).

Minimum values for safety factors are given in the rules for the fatigue strength of propeller hub and pitch mechanism, which includes fasteners of built-up blades. Loading cases concerning fixed-pitch propellers are starting and stopping the propeller, and the rotational load variation in normal operation moving ahead. A safety factor of 1.5 is required when utilizing an analytic calculation method, and a safety factor of 1.3 is required when the calculations are based on a FE model. (DNV 2021c, 15–16.)

Bolts connecting the blades of a built-up propeller to the hub must have tight-fitting threads and be securely locked in place (American Bureau of Shipping 2022a, 343; Bureau Veritas 2022, 184; DNV 2021c, 17; Russian Maritime Register of Shipping 2022, 56).

4 Applying VDI 2230 standard to built-up propeller blade fasteners

The applicability of the VDI 2230 standard for dimensioning bolt joints of built-up propeller blades is studied in this chapter. The standard offers a tool and guideline to carry out bolt joint calculations in practice. The 2014-12 edition of the standard, being available for this study, was utilized. Let it be noted that a more recent 2015-11 edition of Part 1 of the standard, concerning single-bolt joints, has been published (Verein Deutscher Ingenieure n.d.).

In the following, the VDI 2230 standard is first introduced. Initial information required to follow the steps of the standard are then listed. Next, application of the standard in designing the bolt joints of built-up propeller blades is reported following the splitting of the design problem: loading must first be distributed to all bolts within the array and single-bolt joints under the greatest loading need to be evaluated after that. The calculation was implemented by drawing up a Microsoft Excel workbook to use in this specific design task.

4.1 Overview of the standard

The two-part German standard VDI 2230 by Verein Deutscher Ingenieure (VDI, the Association of German Engineers) declares itself as the globally acknowledged principal work for calculating bolt joints. The first edition of the standard was taken into use over 40 years ago and it has been updated with more recent insights since. (VDI 2230-1: 2014, 3.)

VDI 2230-2 (2014, 14) gives the following conditions for the analytical calculation of multi-bolted joints using tapped thread joints:

- Materials must behave in a linear-elastic way.
- Deformations are small and the bolt joint interface is not distorted.
- To avoid large calculation error, a limiting distance between bolt joints and the edges of the bolted pieces is not exceeded.

The standard (VDI 2230-2: 2014, 75) recognizes assembly and operation conditions as two separate loading cases for a bolt joint, each requiring consideration and their common effect

to be regarded in the most unfavorable way. Assembly loading occurs when installing the bolt. Operational loading in the case of this work is the load causing propeller blade loss via plastic bending.

As an input, the calculation procedure given in the standard requires information of the bolt arrangement and the magnitude and type of loading the bolts are to bear. An adequate minimum bolt diameter, the length of required thread engagement and tightening torque are found out as numerical calculation results. The person executing the calculations must be aware that a different number of bolts or just a different placing of the same number of bolts can result in a different requirement for the bolt size – a smaller size for optimally placed ones, and larger for bolts located unfavorably.

VDI 2230-2 instructs the calculation of load distribution among multiple bolts in an array, and VDI 2230-1 treats single-bolt joints. Bolts under the greatest loading are first identified according to the second part of the standard, which considers the load affecting the whole structure.

VDI 2230-1 (2014, 5–6) contains tables for material-specific properties at room temperature. Taking the effects of different temperatures into account in bolt joint calculations is instructed in the standard but they are consciously omitted in the calculation tool devised in this work. Effects of temperature differences, such as thermal elongation, are not among the greatest determining factors, and obtaining adequately precise input for the calculation steps would require further studies. In the calculation tool of only indicative precision, added value of these calculation steps would be questionable. If the tool is experimentally developed further in the future, they could however be added. At that point, true temperature differences, to which a propeller to be designed would be predisposed, would need to be investigated along with the changes of temperature-dependent material properties.

4.2 Required input data

The full list of initial information required from the user of the Excel tool to be developed became evident only after going through all the instructed calculation steps, which are reviewed in the next two sections of this work. However, it is easiest for users of the finished tool to give the required input at once in the beginning. Having looked over the initial

information first it is also easier to understand what is being calculated and what the results are based on. So, the required initial information is listed and categorized here:

- loading
    - magnitude of the operating force
    - direction of the operating force
    - coordinates of the point of force application
- geometric properties of the multi-bolted joint
    - length and diameter of the interface between propeller hub and blade flange
    - bolt locations on the interface
    - smallest outside diameter of the propeller blade flange
- bolt properties
    - modulus of elasticity
    - bolt threads rolled before or after heat treatment
    - necked-down or shank bolts used
    - strength grade
    - custom strength properties if utilized
        - minimum tensile strength
        - minimum 0.2% proof stress
        - shearing strength ratio (shearing strength vs. tensile strength)
- properties of clamped parts, i.e., propeller hub and blade palm
    - minimum coefficient of friction at the interface
    - minimum coefficient of friction in the thread
    - modulus of elasticity
    - tensile strength

    - shearing strength
    - amount of embedding
    - limiting surface pressure
- calculation factors
    - utilization factor of bolt's yield strength
    - reduction coefficient for calculating comparative stress
    - safety margins against shearing off, fatigue failure, slipping, excess surface pressure and exceeding the bolt yield point.

The tightening factor, amount of embedding and limiting surface pressure (the greatest pressure allowed under bolt head, nut or washer) are not automatically solved by the calculation tool but need to be given by the user, who needs to consult tables provided in VDI 2230-1 for determining the quantities.

The structure of the Excel workbook was designed to include each of the following items on their dedicated worksheets:

- index spreadsheet with links to each calculation phase
- input required from the user
- summarizing calculation report with the most important calculated quantities and the results of checks against calculation preconditions
- calculation steps 0–13 following VDI 2230-1 with each step on a single worksheet
- division of the examined load into its components
- distribution of the load among bolts following VDI 2230-2
- table of thread dimensions dependent of the thread nominal diameter
- table of strength properties of different bolt strength grades
- table to select an initial thread size, extrapolated from the standard.

Equations given in VDI 2230-1 include multiple variables dependent of bolt size, i.e., the nominal diameter of the chosen thread. Standard metric ISO-threads are used. The thread list

was formed by extrapolating the VDI 2230-1 (2014, 117) table for bolt diameter selection as allowed in the standard. Threads from M3 to M300 were listed so the size range surely covers the viable options. In the upper end of the size scale, the practicability of tightening bolts with the largest diameters virtually becomes a limiting factor. Big bolts require large tools and great torque. Built-up propeller blades should preferably be mountable even without dry-docking, in which case the working conditions are inherently challenging.

The following thread dimensions were sought outside the standard and tabulated:

- nominal diameter
- thread pitch
- pitch diameter
- minor diameter
- width across flats
- bearing surface outside diameter
- diameter at stress cross-section
- stress cross-section
- minimum bolt cross-section
- clearance hole diameter (medium series)
- minimum bearing area
- height of bolt head.

The studied tables of certain dimensions with no direct calculation formulae provided were limited to a smaller bolt size range than sought after, so some assumptions had to be made. As for the bearing surface outside diameter, standard washer outside diameter was used for sizes M3–M64 and greater sizes were extrapolated. Clearance hole diameters for thread sizes greater than M125 were scaled from the M125 clearance hole. The sum of heights of a standard hexagon head bolt and standard washer was used for the height of bolt head for bolt sizes M3–M64 and larger sizes were extrapolated.

In case of large nominal diameters, utilizing custom bolts with standard threads and individually chosen other dimensions comes into question. An option was implemented in the Excel workbook for the user to choose whether standard dimensions or custom ones are to be used.

4.3 Load distribution within built-up propeller fastener bolt array

The choices regarding which branches of VDI 2230-2 instructions were followed to calculate the load distribution among the fastener bolts of a built-up propeller blade are documented in this section.

The standard (VDI 2230-2: 2014, 19) says that the critical single-bolt joint among all bolts in the array is the first one to fail for any of the following reasons:

- exceeding permissible operating load
- exceeding fatigue strength
- opening of the joint.

Separate bolts in the array may first fail for different reasons, so several bolts possibly need to be examined. Once the critical single-bolt joints are identified, they are to be calculated according to the first part of the standard. (VDI 2230-2: 2014, 19.)

VDI 2230-2 (2014, 15–17) introduces three principal approaches for calculating multi-bolted joints: methods of rigid body mechanics, elastomechanical methods and FEM. Rigid body mechanics is used with the assumption of considerably stiffer clamped components than the bolts used to join the parts together. The standard recommends elastomechanical calculation over rigid body mechanics whenever possible (VDI 2230-2: 2014, 19) and notes that the need for calculation validation by experimenting or FEM is not eliminated by either of the analytical approaches (VDI 2230-1: 2014, 6).

FEM is commonly utilized in propeller design in assessing blade stresses (Carlton 2012, 42; DNV 2021a, 25) and can even be required in case of ice-classed propellers (DNV 2022, 72). In any case, at least a final check by FEM is advisable. The Excel tool developed in this work aims to help speed up the preliminary design of the bolt joints by providing a solution for the bolt arrangement that should be close to what is eventually sought after. Optimally,

a FE calculation would merely confirm that the bolt arrangement examined with the Excel tool is just the right amount on the safe side.

Dimensioning the bolt joints of a built-up blade flange by a method as accurate and reliable as possible instead of a more robust rule provides the benefit that certainty may be had of the adequacy of a lighter structure. The flange and bolts need not be quite as large 'just in case'. The more simplified the calculation method of a complex subject is, the more inaccuracies are necessarily included, which must be compensated by a sufficient safety factor. In other words, part of the 'unnecessary' safety factor can be eliminated by better, more exact calculation. As a result, manufacturing becomes easier and cheaper and besides, a propeller blade design hydrodynamically better in the root area is possible. All this contributes to the business's competitive edge on the market.

VDI 2230-2 (2014, 14) states that the analytical calculation of multi-bolted joint loadings requires making simplifying assumptions, which gives reason to use proper safety factors. On the other hand, calculation results of built-up propeller bolts should in any case finally be confirmed by FEM which allows for smaller safety factors.

As the objective of this thesis is a quick and straightforward calculation tool and not a FE model, a choice had to be made within the VDI 2230-2 standard between the methods of rigid body mechanics and elastomechanics. Rigid body mechanics was chosen to be utilized. Due to its degree of simplification, it is a relatively easy method to apply, but the simplifications must also be remembered when interpreting the calculation results. Before building a propeller with bolts calculated by the tool, validation by FEM is absolutely necessary.

In assessing bolt loads, axial and transverse (shearing) loadings are evaluated separately. The following coordinate system was chosen for the tool following the example of VDI 2230-2:

- x-axis in the left-right (port-starboard) direction
- y-axis upwards
- z-axis in the direction of the propeller shaft line.

The axes are visualized in Figures 7 and 8. The origin of the coordinate system is located in the centroid of propeller blade bolts. To define the centroid, an auxiliary coordinate system

is utilized in which the user of the calculation tool needs to give the coordinates of blade bolts. The origin of the auxiliary coordinate system is in the intersection of the propeller shaft line and aft-side end of propeller hub. Auxiliary (or 'absolute') coordinates are denoted x^*, y^* and z^*. Figure 7 illustrates the directions of the main axes and positive moments about them with a three-dimensional (3D) view. Furthermore, the figure visualizes bolt angle α_i which is measured from the vertical plane and whose use is discussed later, and the components of the force acting on the propeller blade.

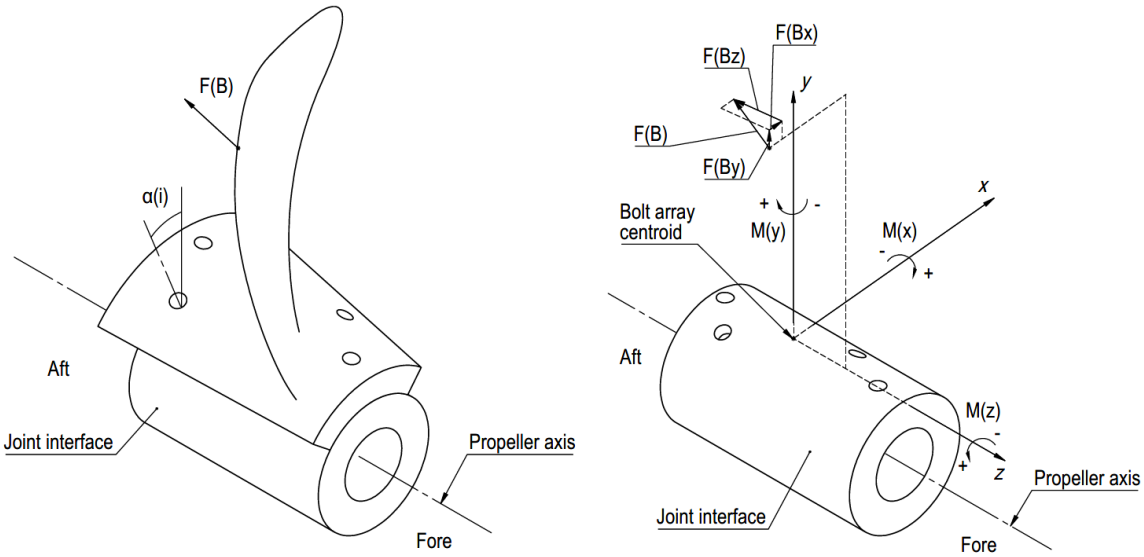

Figure 7. Propeller blade load and its components in the utilized coordinate system with the signs of moments about principal axes shown.

In the rigid body model, the effect of the studied force is divided into moments about principal axes x, y and z. In the normal case of a planar joint interface, transverse bolt loads in the model, besides components of the working load, arise from the moment about the y-axis, denoted M_y. As for axial bolt loads in that case, they are thought to be the combined result of moments M_x and M_z about the horizontal axes. Several different ways of taking the curved geometry of the interface between the propeller hub and blade palm into account were devised and tried in drawing up the Excel tool, considering that the axial and transverse directions vary per bolt.

To calculate the moments about the principal axes, components of the propeller load given by the user must first be solved. Figure 8 illustrates this division into components.

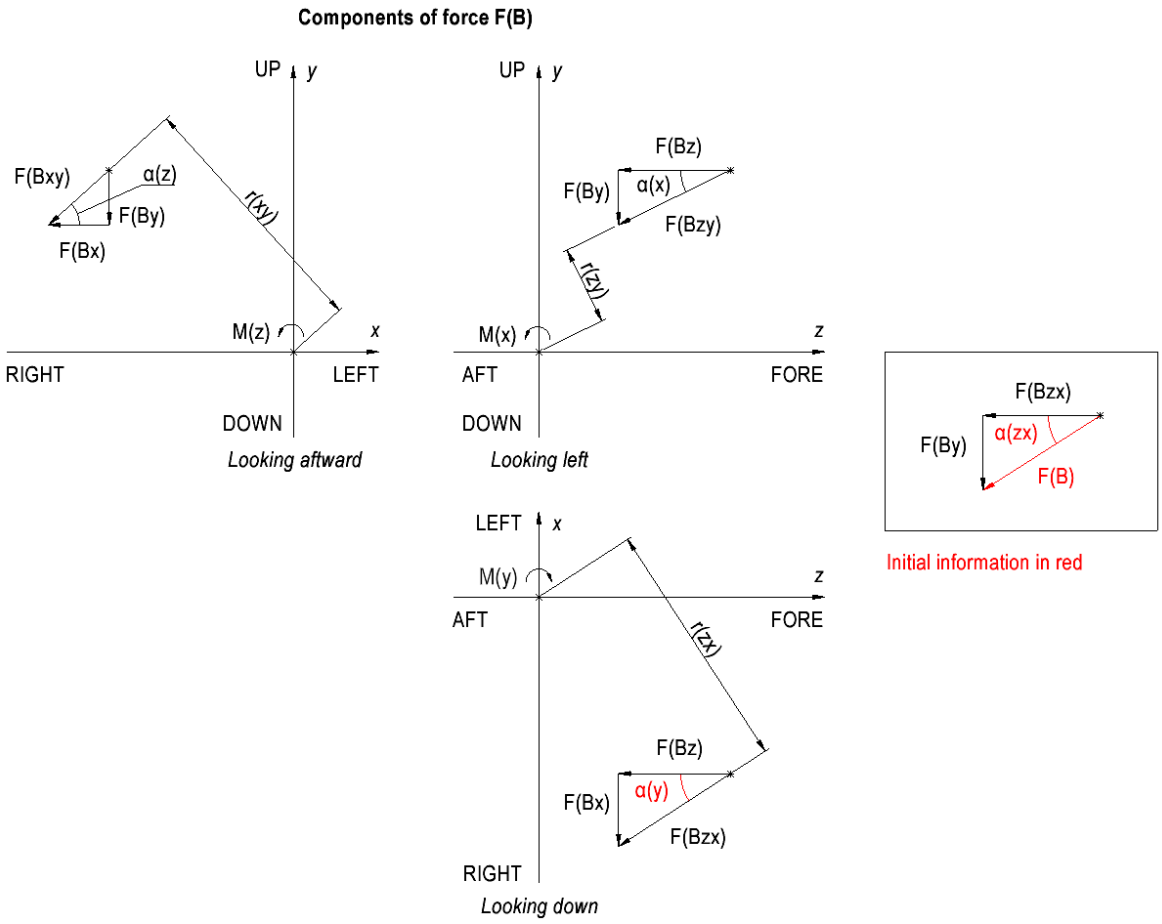

Figure 8. Components of the force affecting the propeller blade.

The following initial information about the load affecting the propeller blade is required:

- magnitude of the force
- coordinates of the point where the force is applied
- direction of the force in relation to the horizontal *xz*-plane
- direction of the force in relation to the vertical *yz*-plane.

The force magnitude is given in kilonewtons. Coordinates of the point of force application are given in the auxiliary coordinate system, and when the locations of all blade bolts are

given and the centroid location is thus determined, the point coordinates are converted to the main coordinate system in the Excel workbook. The direction of the force is defined through angles between the force and the *xz*- and *yz*-planes, marked α_{xz} and α_y (angle around *y*-axis), respectively. From these, the force components in the directions of the principal axes are calculated by trigonometric equations.

Thus, the forces of moments M_x, M_y and M_z are known and additionally their distances from the origin (bolt array centroid) are needed. These, too, are calculated from the coordinates of the point of force application by trigonometry. With the force components and their distances from the origin known, the principal moments are then calculated. These are utilized in distributing the original load between all bolts.

Shearing bolt loads are calculated from the torque M_y in the basic case with a planar bolt joint interface. VDI 2230-2 (2014, 23–25) instructs that the basic procedure in using the rigid body model is distributing the loads in proportion to bolt distances from the centroid, which causes the bolt furthest away from the centroid to be most heavily (transversely) loaded and necessitates a small slipping in the interface. However, in the case of a built-up propeller blade, such slipping is ruled out. Additionally, whether or not a moment both is introduced and exits on the same side (inside or outside) of the bolt array is important (VDI 2230-2: 2014, 91). In the loading case of this thesis, the moment M_y is introduced outside the bolt array at the propeller blade edge and exits inside the bolt array. In such case, according to the standard, the distance of the bolt closest to the centroid, r_{min}, is used in determining the maximum transverse force F_{qmax} acting on a single bolt as follows:

$$F_{qmax} = \frac{M_y}{n_S r_{min}} \tag{5}$$

where n_S is the number of bolts in the array.

For distributing an eccentric axial load among multiple bolts within the rigid body model, VDI 2230-2 (2014, 26) provides the following equation for defining the axial bolt forces $F_{A\,(M)_i}$ arising from the effect of the principal moments M_x and M_z:

$$F_{\mathrm{A\,(M)}_i} = \frac{M_z x_i}{\sum_{i=1}^{n_\mathrm{S}} x_i^2} - \frac{M_\mathrm{x} z_i}{\sum_{i=1}^{n_\mathrm{S}} z_i^2} \tag{6}$$

The sign of the latter term in Equation 6 comes from the choice of directions of the principal axes; positive *x*-axis points left (portside), positive *y*-axis points up and positive *z*-axis points forward as was previously shown in Figures 7 and 8. Thus:

- positive M_x causes upwards force on the aft side and downwards force on the fore side
- positive M_y rotates clockwise seen from top
- positive M_z causes upwards force on the left (port) side and downwards force on the right (starboard) side.

As noted earlier, bolt angle on the surface of propeller hub must be taken into account. In the simplest attempt to do so, the cosine component of the upwards force F_y at each bolting point was considered for each bolt in relation to their angle from the vertical *yz*-plane while the axial bolt load and the transverse load was calculated simply in the same way as with a planar interface without taking the sine component of F_y. Marking bolt angle as α_i (illustrated earlier in Figure 7), the equation below was first used in the calculation tool:

$$F_{\mathrm{A\,(M)}_i} = \cos\alpha_i \cdot \left(\frac{M_\mathrm{z} x_i}{\sum_{i=1}^{n_\mathrm{S}} x_i^2} - \frac{M_\mathrm{x} z_i}{\sum_{i=1}^{n_\mathrm{S}} z_i^2} \right) \tag{7}$$

In the next try, this idea was taken further and the axial and transverse components of forces in the directions of *x*- and *y*-axes were calculated for each bolt. The *z*-direction is in this case perpendicular to all bolt axes. Forces arising from moments about the horizontal axes were calculated by considering the smallest radius from bolt array centroid in the *xz*-plane similarly as in the case of a planar bolt joint interface. As this calculation method, too, proved to result in bolt loads considerably differing from those indicated by FEM, as discussed later, additional alternative calculation methods were tried.

The first of these additional modifications was to consider forces resulting from moments about the principal axes by the true distances between each bolt joint and the centroid in each coordinate plane instead of the minimum radius applied in the previously described calculation attempt. To clarify:

- The working load was first converted to moments about principal axes whose origin lies in the bolt array centroid.
- Forces in the directions of the principal axes resulting from the moments were calculated for each bolting point, considering the true distance between the bolting point and centroid.
- The components of the original working load distributed evenly between all bolts were added following the superposition principle.
- Bolt angles on the curved surface were considered.
    - Axial loads were calculated by adding the axial components of forces in the x- and y-directions.
    - Shearing loads were calculated as the resultant of the perpendicular components of the previously mentioned forces and the force in the z-direction.

A variation considering the minimum radius from the centroid in each coordinate plane in calculating the moments was also tried. Furthermore, both variations were tested with the y-coordinates changed to y^*-coordinates, i.e., the height being considered from the propeller axis plane instead of centroid height. These last modifications assume that the propeller blade would tend to tilt over the propeller axis rather than the centroid and result in smaller calculated transverse bolt loads which, as explained later in section 4.4, define the magnitude of clamp load required in the calculation model utilized.

In determining the required bolt size following VDI 2230-1, the maximum axial load acting on a bolt is needed. The Excel workbook was made to calculate all bolt loads in a table from which the maximum value is easy to pick automatically with an Excel function. The single bolt, or several if that would be the case, most heavily axially and transversely loaded were also visually highlighted to ease the consideration of alternative bolt arrangements.

4.4 Calculating single-bolt joints of built-up propeller blades

The calculation steps of evaluating single-bolt joints of built-up propeller blades are explained in the following account of choices and assumptions made in the process of constructing the Excel calculation tool, but for all the various equations and tables related to each step, the reader is referred to the source standard.

The order of calculations according to the standard is the following (VDI 2230-1: 2014, 29):

0. Nominal diameter
1. Tightening factor
2. Minimum clamp load
3. Dividing the working load
4. Preload changes
5. Minimum assembly preload
6. Maximum assembly preload
7. Assembly stress
8. Working stress
9. Alternating stress
10. Surface pressure
11. Minimum length of engagement
12. Slipping and shearing
13. Tightening torque

The selection of a preliminary bolt size in the calculation step 0 was automated by copying the VDI table into the Excel workbook and extrapolating it as is allowed (VDI 2230-1: 2014, 5) up to M300 from the original greatest thread size M39.

A suitable bolt size is chosen by considering the following (VDI 2230-1: 2014, 117):

- the greatest axial and shearing loads

- the coefficient of friction in the interface between the propeller hub and blade flange
- loading type (static vs. dynamic, concentric vs. eccentric)
- tightening technique.

The automation of searching the table was implemented by the vertical lookup Excel function. With the propeller blade failure load, loading of propeller blade bolts is thought to be static and concentric. The tightening method used at the workshop is considered. It should be noted that more imprecise tightening techniques make a larger bolt diameter necessary and vice versa because of larger scatter in the eventual preload the bolts are tightened to.

In calculation step number 1, a tightening factor is selected from a table in the standard according to the utilized tightening and setting methods (VDI 2230-1: 2014, 31). The tightening factor is used to ensure a proper preload and its values range from 1 to as great as 4 with small values for precise methods and bigger values for more unreliable methods (VDI 2230-1: 2014, 120–121). Presuming a company always uses the same methods in similar bolt joints, the tightening factor is a constant and could be optimized by experimental measurements.

The minimum clamp load required to transmit transverse loads by friction and prevent the opening of the joint or leakage of a sealing surface is calculated in the second step (VDI 2230-1: 2014, 32). Out of these functional requirements, the one demanding a greater clamp load is used as the minimum (VDI 2230-1: 2014, 71). The palm of a built-up fixed-pitch propeller blade does not have a sealing function. Utilizing the rigid body model of VDI 2230-2 includes assuming such calculation factors that the load required for preventing one-sided opening of the joint always ends up being 0. Modifying the rigid body model to determine the minimum clamp load by this criterion instead of friction, which in the current calculation tool is the dominant factor, is a point worth further research in the case of this application.

In the third calculation step, a load factor, load introduction factor and the elastic resiliencies of the clamped parts and the bolt are determined (VDI 2230-1: 2014, 32–33). For a rigid body model, the load introduction factor is 1 (VDI 2230-2: 2014, 20) and the load factor is calculated for concentric clamping and loading. The Excel workbook was made to include an option to use necked-down bolts with the shank without thread reduced to 90% of nominal thread diameter. This is considered in the calculation of elastic resilience. Clamping length,

that is, the thickness of the propeller blade palm, directly affects the elastic resilience of the bolt. In case of conical outer surface of the palm, the clamp length is calculated according to the minor outer diameter to ensure adequate elastic resilience even at the minimum clamp length.

Loss of preload following embedding as well as thermal stress caused by different coefficients of thermal expansion is calculated in step 4 (VDI 2230-1: 2014, 33). The standard contains a table to assess the amount of embedding based on surface roughness of the clamped parts and bolts made of uncoated steel (VDI 2230-1: 2014, 73). Effects of temperature were omitted in this work, but the Excel tool could later be modified to consider them as well.

In steps 5 and 6, the minimum and maximum assembly preloads are calculated, respectively (VDI 2230-1: 2014, 33). This is done in a straightforward way from quantities from earlier steps.

Step 7 is to determine assembly stress and permitted assembly preload and then check whether the bolt size examined thus far continues to serve (VDI 2230-1: 2014, 34). In the case of propeller blades, the standard case of utilizing of 90% of the bolt's minimum yield point is not allowed. In review of classification rules, a factor of 60%–70% was found to be the range satisfying both BV and DNV requirements. Calculations are carried out with the utilization factor of bolt yield strength, 0.2% proof stress of the bolt and minimum coefficient of friction in the thread as input and other quantities being determined by the thread size. The maximum assembly preload calculated in step 6 must not be greater than the permitted preload found in this step. If this condition is not met, a bolt of a larger nominal diameter should be chosen and calculations redone starting from step 2. The user of the Excel tool must be able to make this deliberate choice of bolt size in step 0.

In case a larger nominal diameter does not come into question, the standard (VDI 2230-1: 2014, 34) lists the following possibilities of adjusting the bolt joint design otherwise:

- utilizing a higher strength grade
- tightening the bolts by a different assembly method
- reducing friction
- reducing loading of the joint.

Friction may be affected by choice of materials, and the loading of a single bolt joint can be reduced by relocating bolts or increasing their count. Accommodating bolts of a larger diameter on the palm of a propeller blade may require the enlarging of the propeller hub geometry, which is hydrodynamically unfavorable (Carlton 2012, 449).

In step 8 working stress is determined (VDI 2230-1: 2014, 35), in this work following standard instructions in the case of bolt yield point not being exceeded during loading.

In step 9, alternating stress is checked, and it is required to be below the endurance limit (VDI 2230-1: 2014, 36). Using a rigid body model, the general case (not eccentric) is followed.

Step 10 is to verify that the surface pressure between the bolt head and clamped part is on the safe side of the limiting surface pressure of the clamped part's material in order to avoid creep (VDI 2230-1: 2014, 37). Limiting surface pressures of various materials including several steels are provided in a table in the standard (VDI 2230-1: 2014, 122–123).

In step 11, the minimum required length of thread engagement is determined for the purpose of ensuring that the bolt joint will not fail by stripped threads (VDI 2230-1: 2014, 37). The calculation in the tool is simplified by not considering thread tolerances, while the standard (VDI 2230-1: 2014, 100) considers the most unfavorable case with the bolt thread outer diameter at the lower tolerance limit and the pitch flank diameter of the internal thread at the upper limit.

Knowing the minimum required length of thread engagement, the total bolt length can be defined by adding the maximum clamp length. It should be made sure that the bolt fits within the blade flange and hub at the end of minor outer diameter and does not extend into the propeller shaft all the way through the hub. The maximum clamp length can be adjusted by having two different interface diameters and a step in the interface. This way, the bolts, assuming an identical length, need not be so long and there is also a more uniform palm thickness along the length of the interface. Additionally, the step between the two hub diameters can help in positioning the blade before fastening the bolts.

In step 12, safety margin against slipping and shearing stress is established and in the final, 13th step, the tightening torque for a torque-controlled tightening method is calculated (VDI 2230-1: 2014, 37–38).

The Excel workbook was designed to include a summary sheet, on which the calculated main dimensions and conclusions are provided. The sheet lists the nominal diameter chosen for the bolt joint, the length of required thread engagement, total bolt length and the tightening torque. The results of checks in calculation steps 7–10 for bolt size, yielding of bolts, fatigue failure and exceeding the allowed surface pressure are shown as well to not accidentally use a bolt that has been found inadequate during the calculations.

The suitability of the chosen bolt size (nominal diameter and length) should finally be confirmed by making sure that all bolts have room to move in and out of their holes without interfering with the propeller blade and that the tightening tools fit in place.

5 Results

The finished calculation tool was tested with data from an existing exemplary model of a built-up propeller. Propeller and bolt material data, bolt locations and other required input were given into the calculation tool, and the results were compared with values extracted from a FE model. In the chosen propeller design, the blade bolts are custom-dimensioned and not standard; however, both FEM and the Excel calculation tool are capable of taking the custom dimensions into account. Test input, resulting output and comparison of results against finite element analysis (FEA) are recounted in the following.

5.1 Test input

Most of test input is presented in Table 1. Bolt locations used in the calculations are given in Table 2, and user-given selection of bolt diameter and thread pitch are shown in the resulting calculation report in Table 3.

As the utilized FEA software requires the user to define the preload, 2 000 kN was used in each loading case. The Excel calculation tool calculates preload by itself. In it, the magnitude of the preload depends on the working load.

Table 1. Test input values.

Loading			
F_B =	6 850	kN	Operating force in any direction acting on a connecting point
x_F^* =	-980.3	mm	Point of force application measured from vertical propeller axis plane
y_F^* =	1 509.6	mm	Point of force application measured from horizontal propeller axis plane
z_F^* =	935.5	mm	Point of force application measured from aft-side end of propeller hub
α_y =	180	°	Angle between F_B and vertical *yz*-plane (around *y*-axis)
α_{xz} =	0	°	Angle between F_B and horizontal *xz*-plane

Table 1 continues. Test input values.

Joint geometry			
$D_{f\,min}$ =	1 431	mm	Smallest outside diameter of propeller blade flange
D_{hub} =	1 080	mm	Propeller hub outer diameter
l_{Gew} =	0	mm	Length of the free loaded thread
l_{hub} =	1 023	mm	Length of (contact surface between) propeller blade flange and hub in the direction of propeller axis
n_S =	8		Number of bolts
Bolt material properties			
E_S =	200	GPa	Young's modulus of the bolt material
Grade:	12.9		Bolt strength grade
Rolled:	After heat treatment		Bolt threads rolled before or after heat treatment
Shank:	Necked-down		Necked-down or shank bolts used
Propeller material properties			
E_P =	200	GPa	Young's modulus of the clamped parts
f_Z =	8	µm	Plastic deformation as a result of embedding, amount of embedding
p_G =	630	N/mm^2	Limiting surface pressure, maximum permissible pressure under bolt head, nut or washer
R_{mM} =	750	N/mm^2	Tensile strength of the nut
$\mu_{G\,min}$ =	0.14		Minimum coefficient of friction in the thread
$\mu_{T\,min}$ =	0.15		Minimum coefficient of friction at the interface during combined loading
τ_{BM} =	450	N/mm^2	Shearing strength of the nut
Calculation factors			
k_τ =	0.5		Reduction coefficient
S_A =	1.1		Safety margin against shearing off
S_D =	1.0		Safety margin against fatigue failure
S_F =	1.0		Safety margin against exceeding the yield point
S_G =	1.0		Safety margin against slipping
S_P =	1.0		Safety margin against surface pressure
v =	90 %		Utilization factor of bolt yield point $R_{p0.2min}$
α_A =	1		Tightening factor

Table 2 lists the bolt positions of the studied built-up propeller blade. The y_i^*-coordinate is calculated by the Excel tool.

Table 2. Bolt positions.

Bolt i	x_i^* [mm]	z_i^* [mm]
1	0.0	923.0
2	184.7	923.0
3	309.7	796.0
4	309.7	546.0
5	0.0	96.0
6	-184.7	96.0
7	-309.7	196.0
8	-309.7	446.0

The test calculation was carried out five times with increasing loads defined to act on the propeller blade. The test load magnitudes for each calculation round are presented in Figure 9.

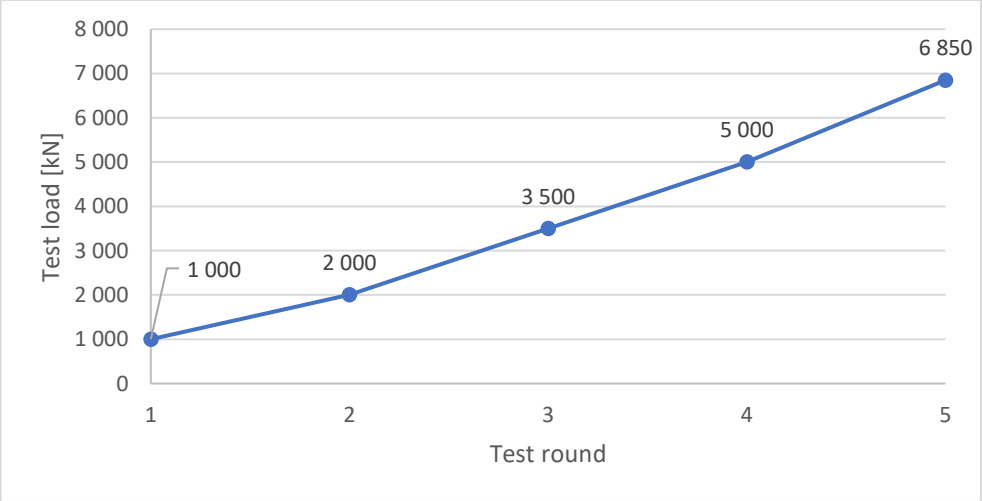

Figure 9. Test loads on the propeller blade.

The operating force – from 1 000 kN to 6 850 kN as shown in Figure 9 – was defined to affect in the aft direction in parallel with the propeller shaft line. The point where the force was directed was chosen to be the leading edge of the propeller blade at a distance equal to 0.8 blade radius from the propeller shaft line. The coordinates for the point were measured from the 3D model. A schematic visualization of the point of force application was presented earlier in Figure 7 in section 4.3.

The studied built-up propeller design utilizes eight bolts. As a simplifying assumption with only a marginal error to the safe side, bolt threads were assumed to perfectly mate with hole threads, so the interface of the bolt shank and thread would be exactly at the threaded hole edge. Necked-down bolts were used, with the bolt shank without thread reduced to 90% of bolt nominal diameter. Threads were chosen to be rolled after heat treatment, because then the bolts' stress amplitude of the endurance limit is higher than that of bolts with threads rolled before heat treatment meaning greater safety against fatigue failure. However, the propeller blade failure load is not a fatigue load but the greatest once-in-a-lifetime load that is to be expected for the bolts. If the calculations indicate fatigue failure under the blade failure load, the bolts need not necessarily be rejected, but fatigue should be assessed with a smaller load determined separately.

The amount of embedding, limiting surface pressure and coefficients of friction were looked up from tables of the VDI standard. The FE model was configured to utilize the same coefficients of friction and similar material properties.

As for the calculation factors, the value recommended by VDI in the standard was used for the reduction coefficient applied in examining the working stress. All safety margins were defined to be minimal for simplicity in this test case. 90% utilization of bolt yield point was allowed, although classification societies in reality only accept a lower percentage, as mentioned earlier. A high utilization percentage was chosen as it occurred that there is significant difference between the results of Excel calculations and FEA. The reasoning behind this justification is that adjusting the utilization of bolt yield strength is fine-tuning that can be done after more reliable results can be gotten from the tool. Since corrections turned out to be necessary at a coarser level, the standard default value of 90% was deemed appropriate at this stage.

For simplicity, the tightening factor was defined to be an ideal 1, which means that the defined preload can be achieved precisely. With precise tools and methods, the tightening factor can have as low a value as about 1.1, and in the other end it can be even 4 (VDI 2230-1: 2014, 120–121). The required minimum preload is multiplied by the tightening factor to define the maximum design preload which the bolts must endure. The tightening factor accounts for imprecision in setting the preload and ensures that after aiming at the maximum preload, at least the required minimum is reached.

5.2 Results of test calculation

The calculation tool gives a report like the one presented in Table 3. The result shown is for the greatest studied operating force of 6 850 kN.

Table 3. Output of the test calculation.

Examined bolt: Custom M100x4			
d_{pro} =	110	mm	Proposed bolt diameter
d =	100	mm	Bolt diameter = outside diameter of thread (nominal diameter)
P =	4	mm	Thread pitch
Custom bolt dimensions			
d_h =	107	mm	Clearance hole diameter
d_W =	142	mm	Bearing surface outside diameter
k =	70	mm	Height of bolt head
Calculated bolt quantities			
l_{min} =	190	mm	Minimum total bolt length
m_{ges} =	82	mm	Total length of thread engagement
M_A =	107	kNm	Tightening moment during assembly for preloading a bolt*
Calculation check results			
			Elastic resilience and load factor
			Successfully calculated
			Bolt size check
			Bolt failure in preloading
			*Note! Next steps only assume permissible preload
			Working stress*
			Yield safety margin OK
			Alternating stress*
			Fatigue safety margin OK
			Surface pressure*
			Too much surface pressure in assembled state
			Too much surface pressure in working state
			Slipping and shearing*
			Risk of slipping
			Shearing safety margin OK

The calculation tool suggests a bolt diameter of 110 mm, but nominal diameter 100 mm with a pitch of 4 mm was chosen according to the test propeller design. User-given custom bolt

dimensions can be seen in Table 3 as well; in this case, the bearing surface outside diameter and height of bolt head are not standard.

The tool calculates the required length of thread engagement, adds it to the clamp length and rounds the result up to give the total minimum bolt length too. The tightening moment is reported as well.

After numeric quantities, the check results of relevant calculation steps are reported verbally. Elastic resilience and load factor are calculated first and required by subsequent calculation steps. Hence the success of this step is verified; it can fail because of an erroneous combination of input data, such as the bearing surface of a bolt not being completely on top of propeller blade palm.

Bolt size check is carried out by comparing the required preload with preload permissible for the bolt. In the test case, bolt failure in preloading is reported, which means a preload greater than permitted for the bolt is necessary for the bolt joints to function correctly. In all calculation steps following the bolt size check, the permissible preload – being the most demanding possible condition – is used in the calculations. This is highlighted in the results of the tool if the bolt size check fails. The tightening moment is also calculated using the allowed preload, not the required preload which may end up exceeding the permitted value.

With the previously mentioned note of caution and considering the allowed preload, the Excel tool states the yield, fatigue and shearing safety margins to be met and warns about too great surface pressure both in the assembled and working states, and about the risk of slipping in the test case.

The conclusion that would have to be made from the calculation report in a real design process is that the studied bolt arrangement is not satisfactory. A bigger nominal diameter or a different arrangement, considering both the number and placement of bolts, would need to be examined.

5.3 Comparison with finite element analysis

To test the validity of the newly developed Excel workbook, its calculation results were compared with data from a FE model constructed with Ansys 2023 R1 software (Rauti 2023). Figure 10 illustrates the 3D model used in the validity study. The blade needed to be

cut at the radius where the working load was directed for meshing to succeed, but this was presumed to not alter the distribution of loading among bolts considerably.

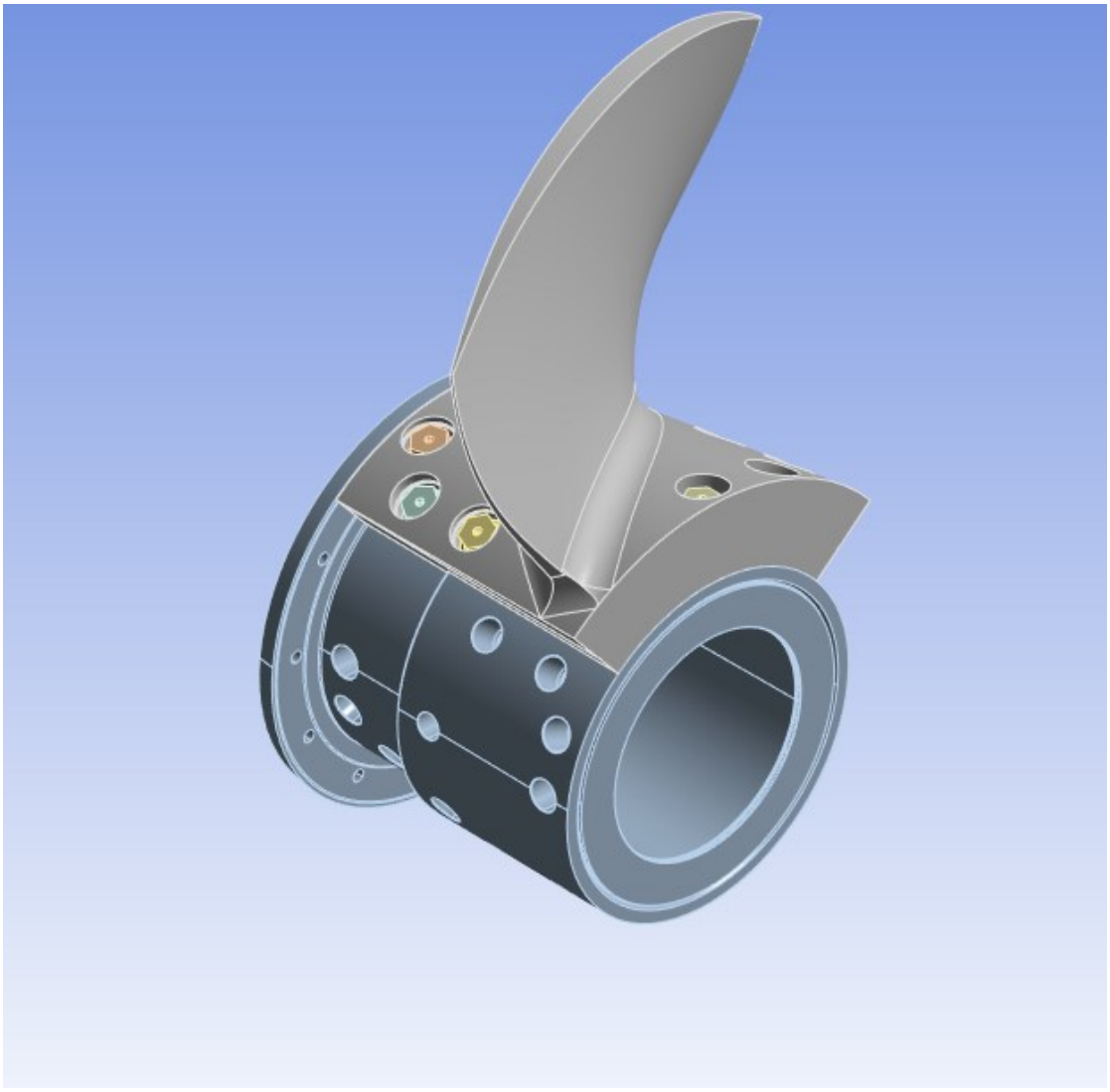

Figure 10. 3D model of the test propeller used in FEA (Rauti 2023).

Figure 11 shows the bolts in the FE model under sole preloading without additional external loading. This situation occurs after assembly. With the preload given for the test model, the bolts seem to have a stress concentration at the root of bolts' bearing surface.

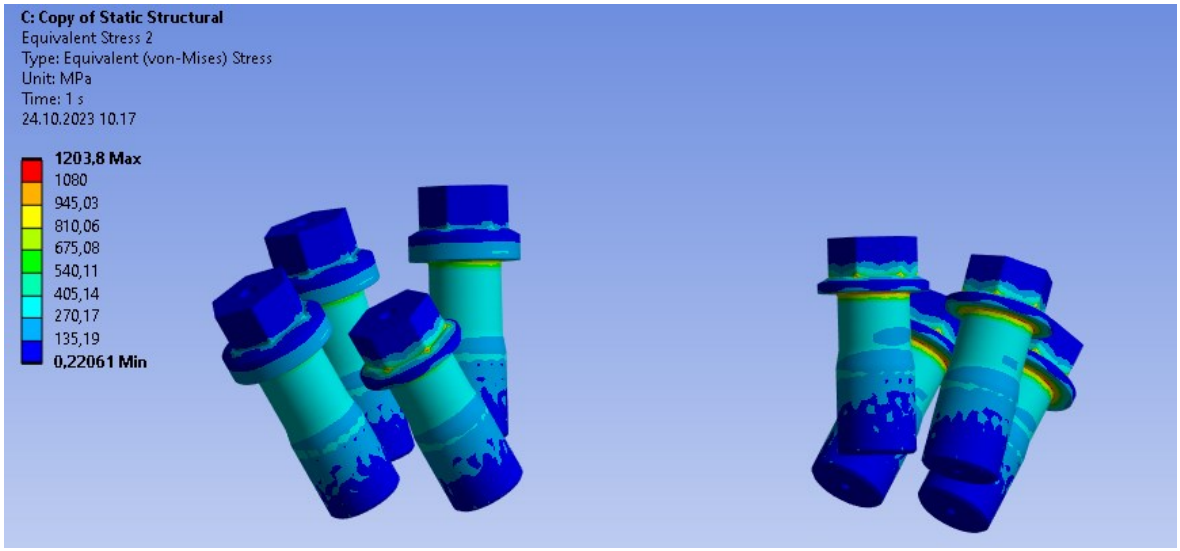

Figure 11. Bolts of FE model under preloading (Rauti 2023).

Figure 12 illustrates what the bolts look like in the FEA software under excessive external loading resulting in bolt failure. The figure presents the situation before the bolts visibly yield and deform under too much stress. With more loading added, the bolt with the red shank will stretch.

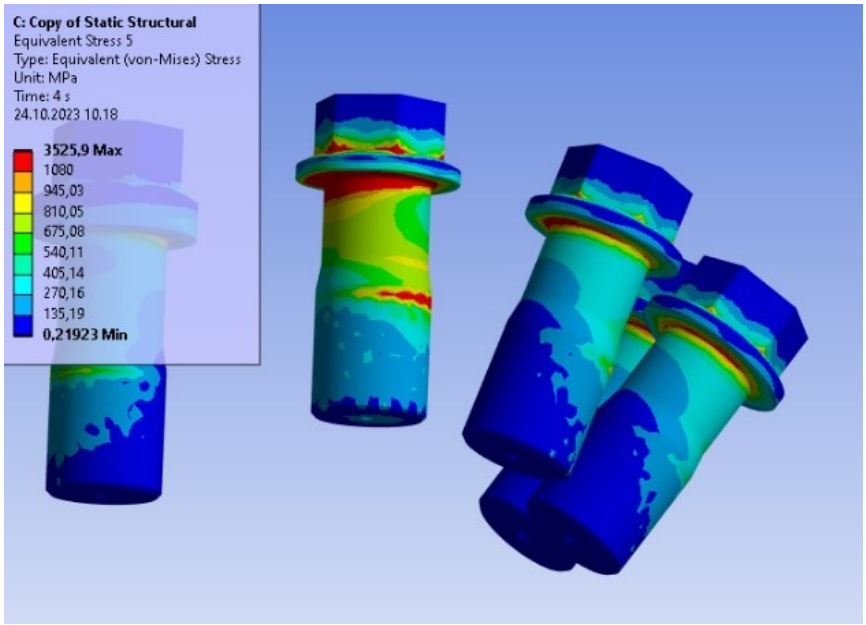

Figure 12. Bolts of FE model under excessive loading causing bolt failure (Rauti 2023).

The Excel tool calculates axial and transverse loads for each bolt. These interim result values were compared to axial reaction forces given by the FE model. The comparison results are visualized in Figures 13 and 14, which show the relationship Excel value per FEM value in each case of different external loads applied to the propeller blade. FEM values of Figure 13 were obtained from the model configuration without contact in the interface step, representing a single cylindrical joint interface, and Figure 14 presents results from the model with contact in the step. The Excel tool does not consider the existence of the step, so the same Excel results were compared to two different FEM values. Attempt 1 in both figures, printed in gray and located higher on the figure scales, represents the initial simplified calculation of load distribution described in section 4.3. Attempt 2 represents the modified calculation method developed further, the procedure of which is explained at the end of section 4.3.

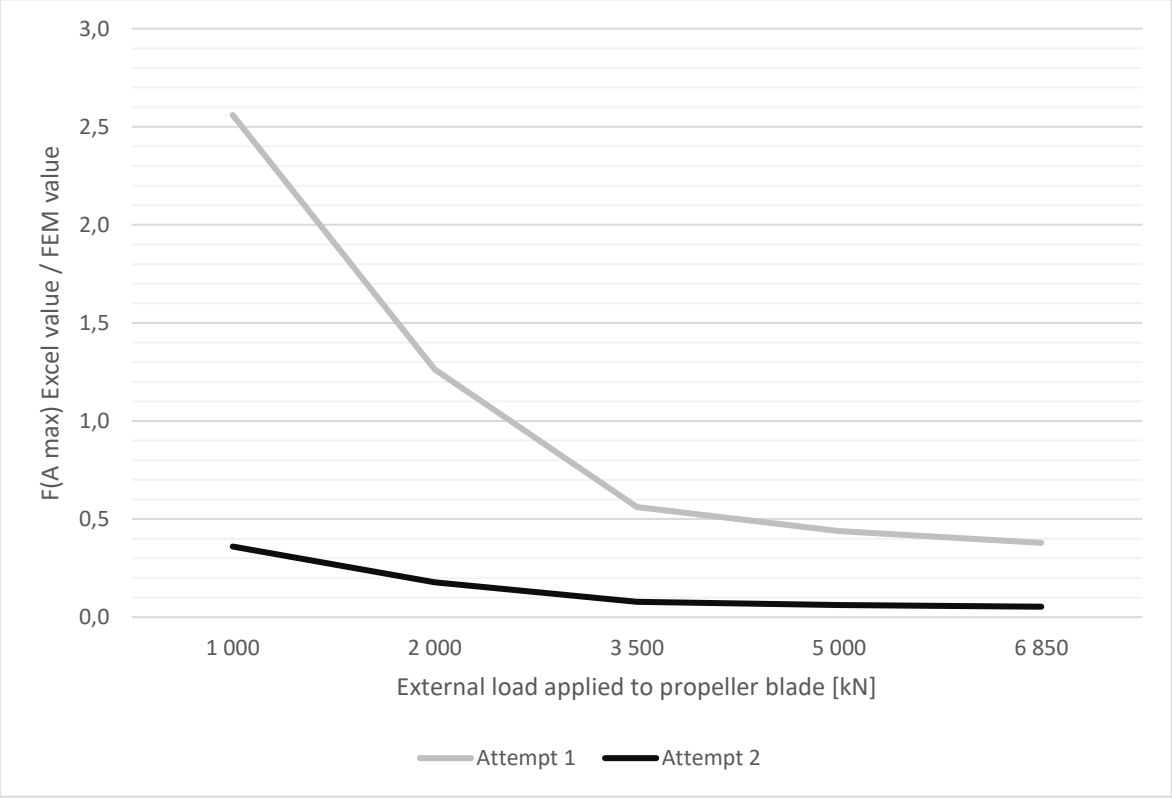

Figure 13. Axial bolt load calculated by the Excel tool per value extracted from FE model with curved joint interface without step.

In the comparison it quickly becomes apparent that there are significant differences. With small external loads, maximum axial bolt loads calculated by the Excel tool utilizing the simplest method (Attempt 1 in Figures 13 and 14) are greater than by FEM, and with greater external loads, the situation changes to the opposite. In other words, when a small external load is given for the propeller blade, the Excel tool seems to exaggerate the maximum axial load coming to the most loaded bolt by a factor greater than two and in the other end the tool appears to report a value that is less than half of the actual axial load. With the more complex calculation method (Attempt 2 in the figures), the Excel results always end up being smaller than what FEM reports and they would need to be multiplied by a factor of about 3–20 to match. The range is too broad for a simple correction factor to be able to be reliably established by this data.

Figure 14 presenting the comparison with the FE model in which the step is considered present is very alike with the previous Figure 13. The scatter of differences between Excel and FEM results seems a little smaller in this case, but it is still notable, and the graphs have a similar form.

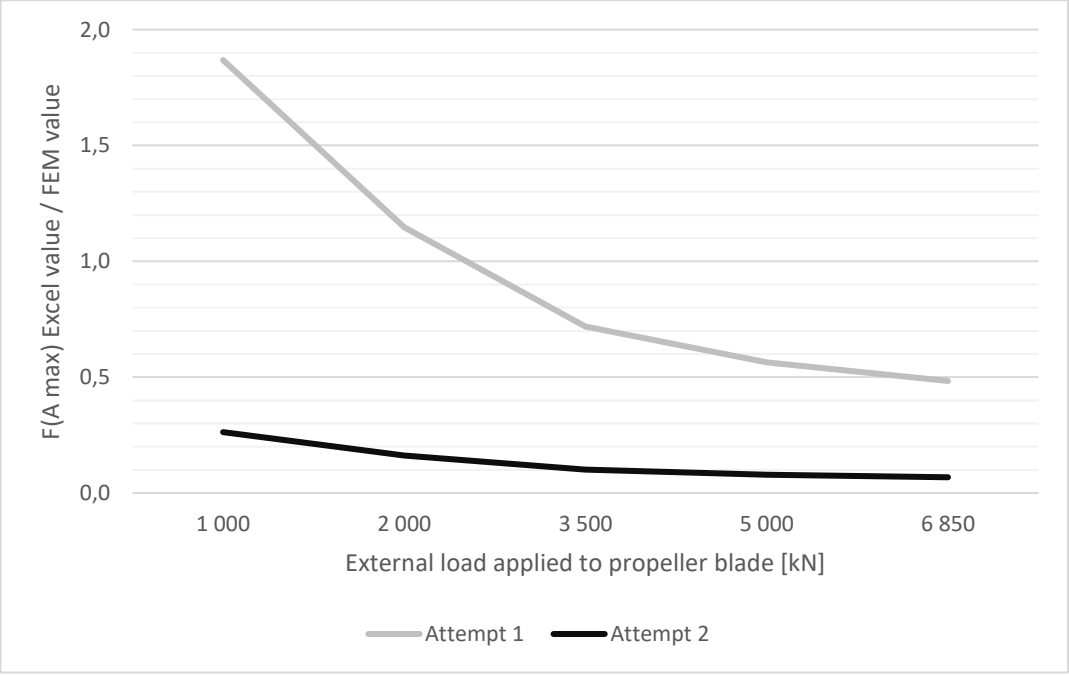

Figure 14. Axial bolt load calculated by the Excel tool per value extracted from FE model with curved joint interface and step.

A difficulty in comparing the results lies in the fact that for the FE calculations, a preload needs to be separately set, whilst the Excel tool following VDI instructions defines the preload for each loading case according to the working load.

A preload lower than indicated necessary by the Excel tool was utilized in the FE model because the suggested value seemed to cause bolt failure in the assembly stage and the simulation would not get to the stage where external loading is added for the propeller. The Excel calculator predicted a similar outcome, but its method of distributing loading among the bolts in the array needs further studies. That phase in the beginning of the calculation process is very important because it provides the input values onto which all subsequent results, including the required magnitude of bolt preload, are based. Several different propellers with different bolt arrangements should be examined when undertaking this development task.

In the calculations of the Excel workbook following VDI standard instructions, the neutral axis of the bolt arrangement was chosen to be located at the bolt array centroid. To assess whether this seems reasonable and correct or not, the distribution of surface pressure in the joint interface was observed from the FE model.

Figure 15 shows the surface pressure distribution in assembly conditions, under preloading without any additional working load. In the assembly conditions, there is surface pressure around the bolts but not on areas far away from them.

The bolt joint interface and the step in it are well visible in Figures 15–17. To study the effect of the step in the distribution of loading among bolts, two variants of the model were utilized. In one configuration, contact was defined between the step surfaces (perpendicular to the cylindrical surfaces) of the propeller blade palm and hub, and the other was defined to not have that contact. The surface pressure distribution turned out to behave in a similar manner with and without the step, although bolt loadings ended up being smaller with the step.

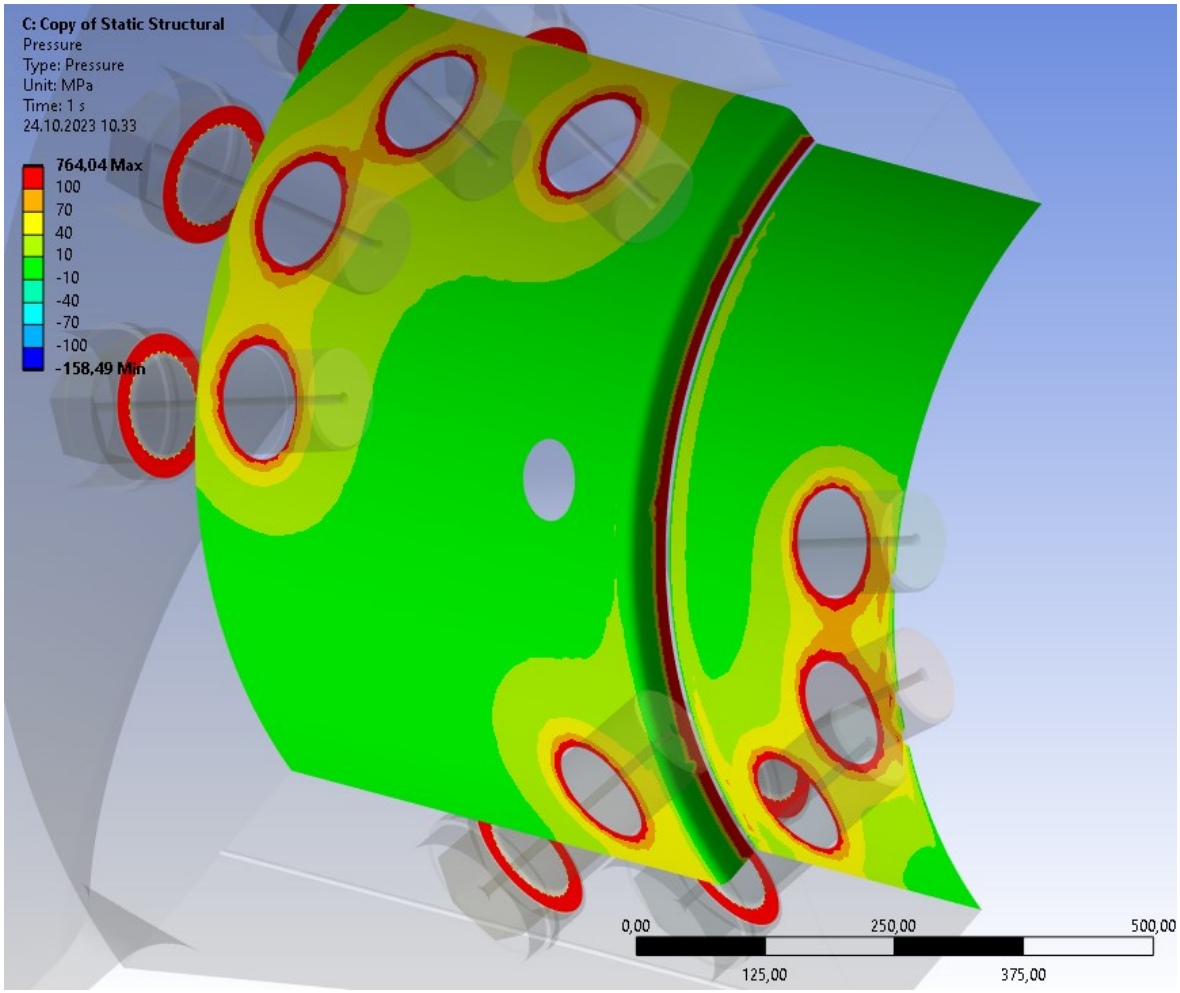

Figure 15. Surface pressure under preloading (Rauti 2023).

In Figure 15, there seems to be great surface pressure on the outer edge of the step surface. That would not necessarily be true for the assembly conditions of a real propeller but could be because of the propeller hub surface being defined fixed in the FE model. The propeller blade palm may tend to bend inwards under preloading in the model.

Figure 16 shows the distribution of surface pressure when some external loading is added to the model. Now one bolt has failed, as contact at the bolting point has been lost and there is no surface pressure left in that area. The second bolt is also similarly failing, and the multi-bolted joint is opening where surface pressure has been lost compared to the initial state shown in Figure 15. From the viewpoint of evaluating a bolt joint design, this kind of situation would be unacceptable. It can be seen in Figure 16 that there is additional surface pressure around all the remaining bolts and especially around the bolts in the opposite edge.

Additionally, there is some surface pressure on a larger area further away from the bolts, and the sides of tension and compression are apparent. The limit between these two sides appears to pass quite near the approximate location of the bolt array centroid, so assuming the position of the neutral axis there seems reasonable. Calculating the load distribution in the Excel tool was tried by moving the neutral axis to the propeller axis plane, but the notions made from FEA suggest that some other measures to correct the calculations should be considered.

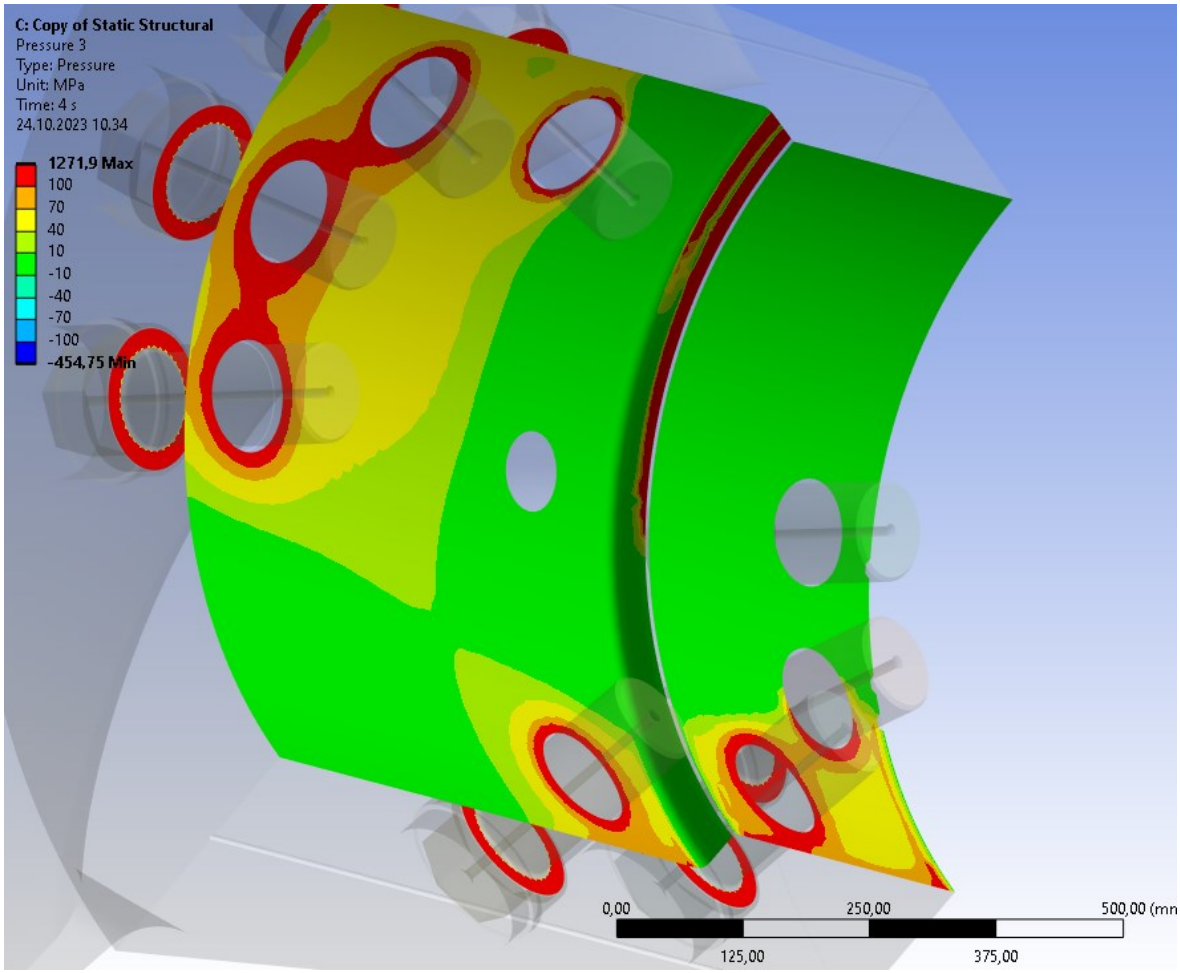

Figure 16. Surface pressure under preloading and a force of 3 500 kN acting on the test propeller blade (Rauti 2023).

Surface pressure in the planar step interface is shifting to one end in Figure 16 and even more so in Figure 17 in which the first bolt on the other side of the propeller blade has failed too.

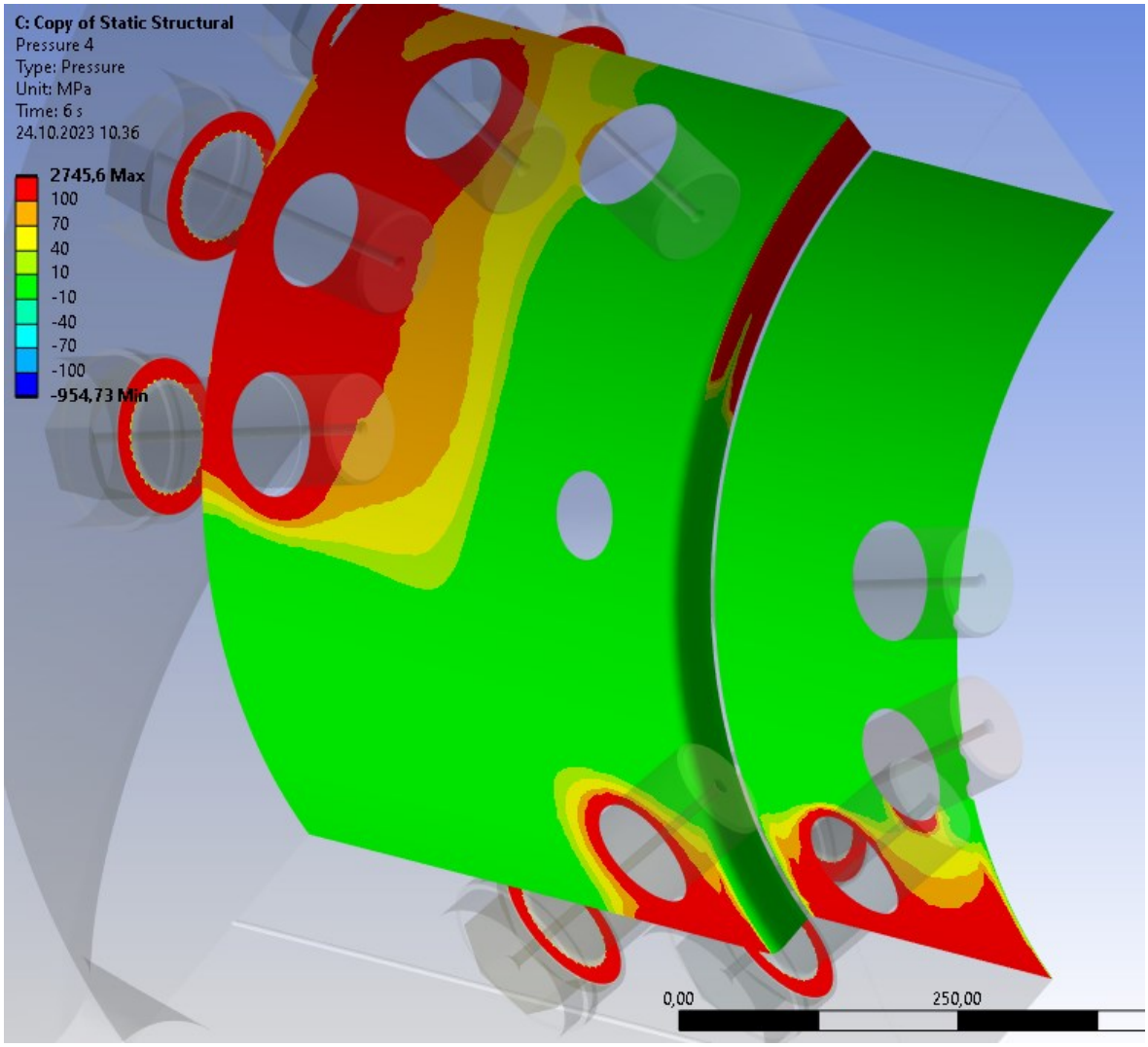

Figure 17. Surface pressure under preloading and a force of 6 850 kN acting on the propeller blade (Rauti 2023).

The distribution of surface pressure was similarly observed in the case of a flat blade palm. The original test propeller blade was modified by modeling a new planar blade palm whose dimensions in relation to the blade were taken from the middle of the curved blade palm.

Figure 18 shows images of the modified 3D model configured both with and without the step in the interface. This model is simplified to some extent; bolt locations were kept identical with the original, looking down along the *y*-axis, and the blade root was left without a fillet for this study.

With the joint interface flattened this way, bolts ended up being so close to each other that in reality this could not be allowed and the blade root fillet would surely interfere with the bolt holes. However, the models are usable in the purpose of comparing surface pressure distribution in the cases of a flat and curved interface.

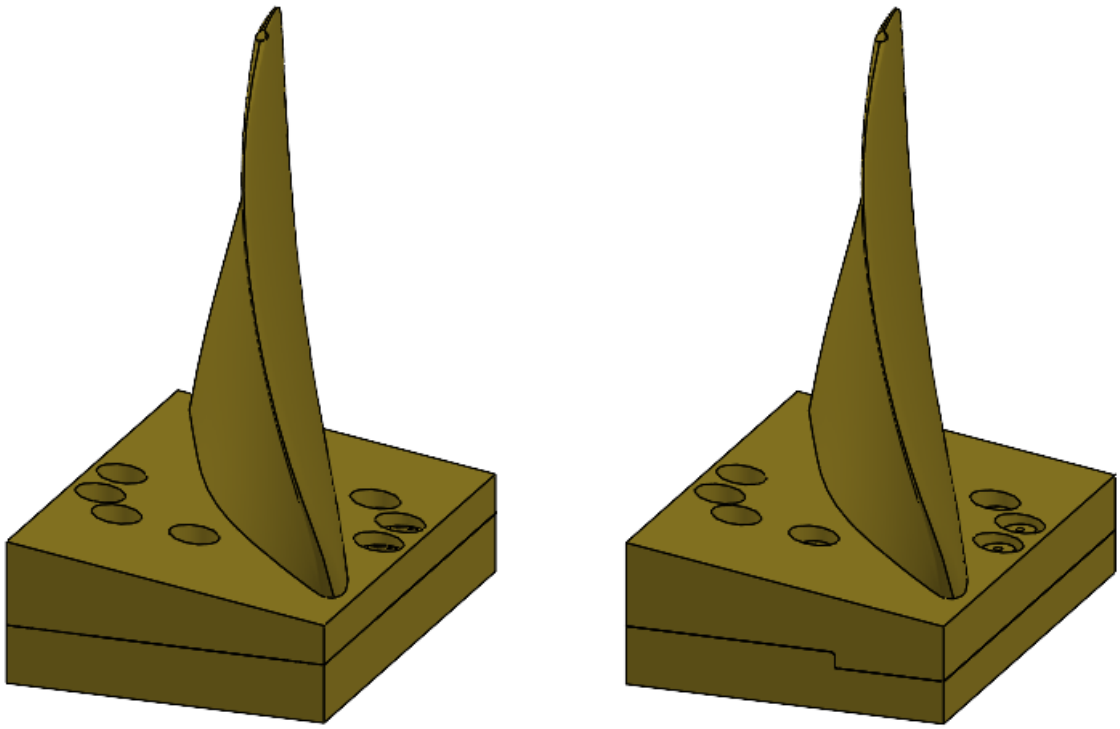

Figure 18. Propeller blade with joint interface modified to be planar, with and without step.

Surface pressure distribution under preloading without an external load is shown in Figure 19. The model shown is without the step in the interface. The surface pressure distributions were similar in both cases, with and without the step.

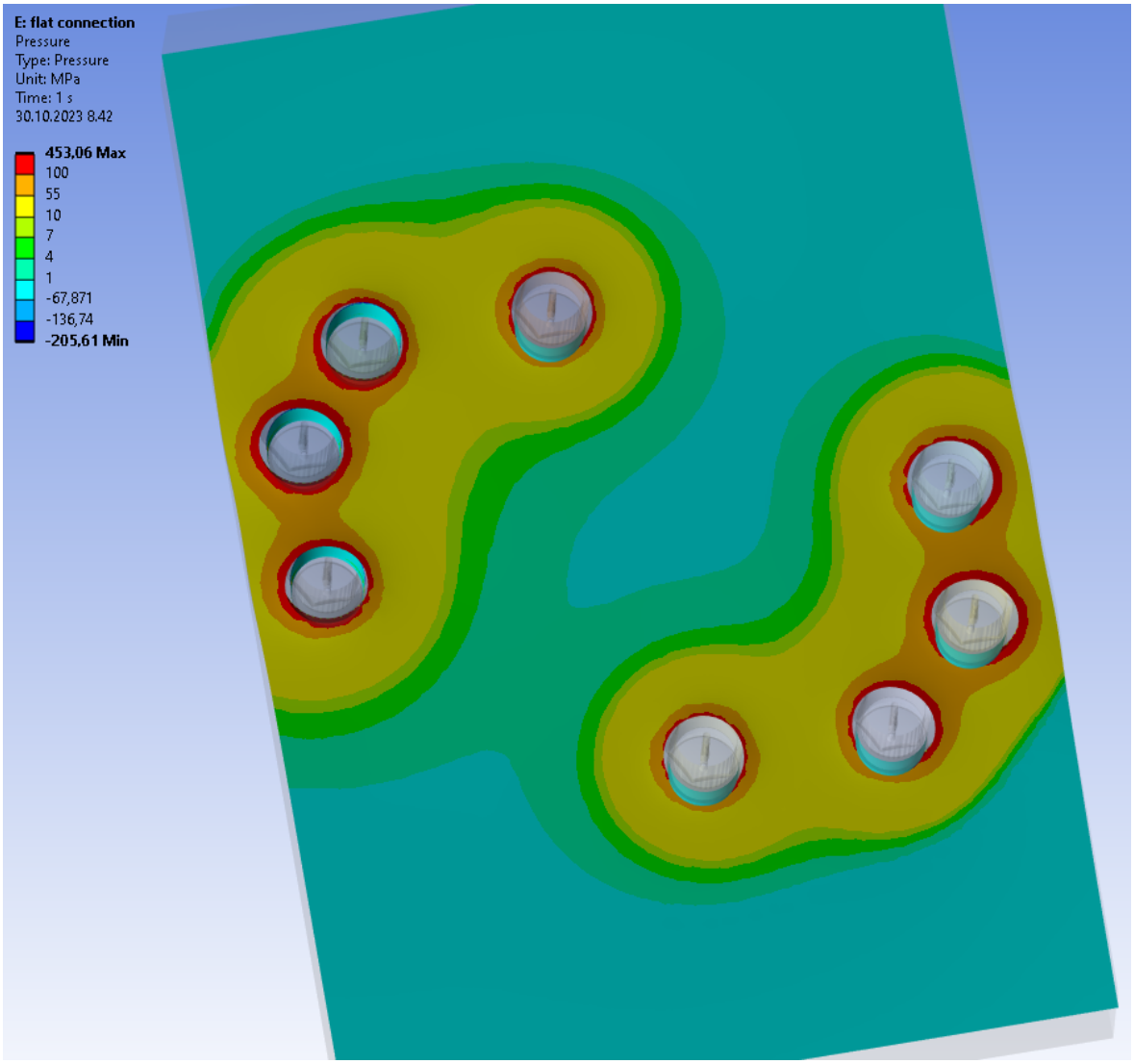

Figure 19. Surface pressure of flat interface under preloading (Rauti 2023).

Figure 20 shows how the surface pressure changes when external loading is added. In this case, the limit between areas with and without additional surface pressure passes through the approximate location of the bolt array centroid even more clearly than in the case of a curved interface previously shown in Figure 16. This is expected, as a flat interface is much simpler and more common in bolt joints, and simplification of a multi-bolted joint by a rigid body model following the VDI 2230 standard instructions applies better.

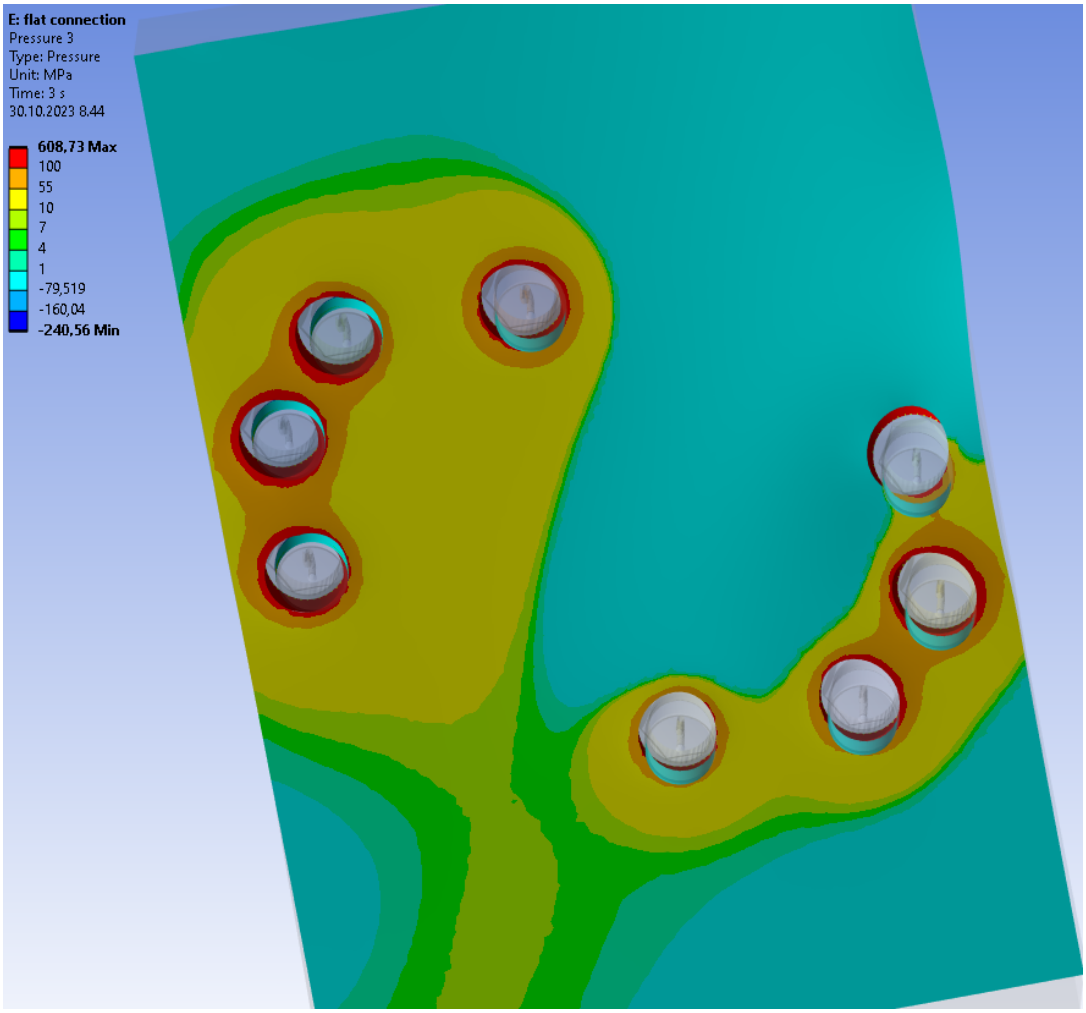

Figure 20. Surface pressure of flat interface under preloading and a force of 2 000 kN acting on the propeller blade (Rauti 2023).

In Figure 20, the first bolt has failed and contact around it has been lost. According to the FE simulations run, the models with a flat interface did not endure as great loads as the models with a curved interface did but the clamped parts were separated sooner.

Results presented here were gathered from studying a single arrangement of a specific design and cannot be generalized, although some slight variations of the original design were reviewed. The application, however, is a concrete one, and validating a properly functioning calculation tool after additional research would be most valuable and helpful in designing bolt joints like the ones studied in this work. Finding a reliable way of determining how loads are distributed among several bolts on a curved surface is a necessary step to that end.

6 Discussion

In the course of this work, the design process of built-up propeller bolt joints was outlined. An illustration of the process is presented in Figure 21. The figure describes how propeller geometry and the workshop environment where the propeller is assembled are input for the bolt joint design phase. The propeller hub, in turn, affects propeller geometry. Dimensions involved in determining bolt joints are set in the designing of each of the two propeller parts.

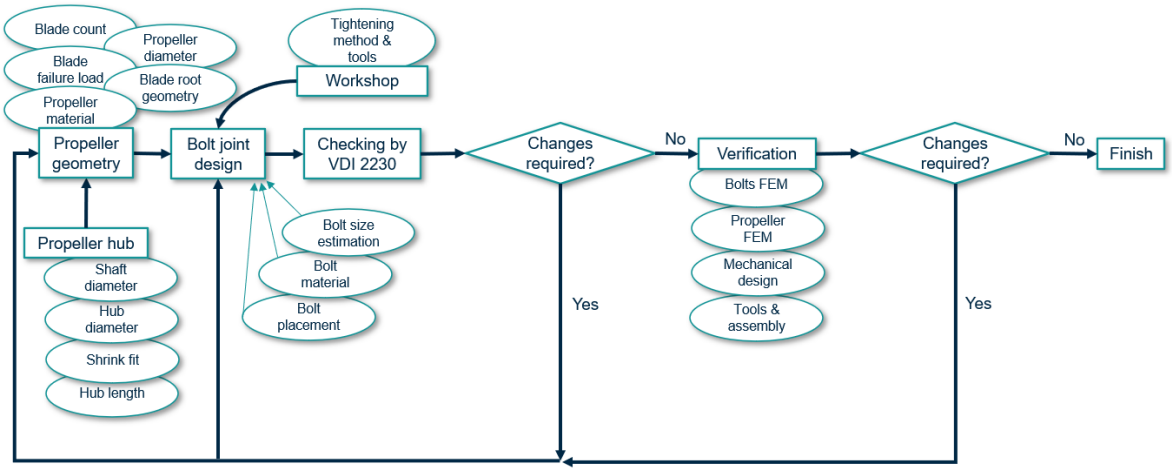

Figure 21. Design process of built-up propeller bolt joints.

The key in designing the propeller hub is the shrink fit by which it is installed onto the propeller shaft. The shaft diameter, hub diameter and hub length are determined, and thus, the material thickness available for threaded holes is known. Propeller blade and palm properties are determined on top of the hub: blade count, propeller diameter and blade root geometry. These define and limit the space available for placing the bolts. The blade failure load is also determined in this propeller design phase. The material choice of both the propeller and the bolts is important. As for the workshop, the tightening method and tools utilized are considered in the tightening factor as explained in section 4.4.

In Figure 21, the bolt joint design and checking against the VDI 2230 standard are the phases addressed by this work and the Excel tool developed. Bolts are placed and their size and material defined in this phase. If bolts are calculated to fail, the arrangement is modified and

the check reiterated. If modifying the bolts or their material or placement does not solve the issue, changes may be necessary at an earlier stage in propeller design.

Ideally, once calculation according to the VDI standard indicates a satisfactory bolt joint, this is verified by FEM. Again, it is possible that changes and a recheck may be needed. In the last checking phase, it should also be ensured that the manufacturing and installation of the design is possible. After this, the process is finished.

Without a calculation tool to which to resort before FEM, the process would go to FEM straight from propeller design. Then studying the effects of modifications can be slower and burdensome, as FE calculations may take time. On the other hand, the bolt arrangements of separate propellers may well turn out quite similar and it becomes easier to start with good estimates with experience accumulated from multiple propellers.

Notable differences were found between the results given by FEM and the Excel workbook devised in this work. Most likely FEM is much closer to reality than the Excel tool at its current state. For the workbook to be usable, some further research and tuning of the tool is necessary. Because of the differences between results gained via FEM and the Excel tool, the calculation of load distribution was tried with several different approaches which are documented in section 4.3.

Calculating a single-bolt joint following the VDI 2230 standard is relatively simple compared to multi-bolted joints and distributing loadings among a bolt array. Calculations done according to VDI 2230-2 yield required input information for the calculation of single-bolt joints. It is evident that in this work, the problem in the calculations arises from the division of loading between bolts. The rigid body calculation model utilized cannot account for the effect of the curved shape of the joint interface, nor a step in the interface. Based on the surface pressure distribution in the FE model, the assumption of the neutral axis passing through the bolt array centroid seems reasonable, however.

There is also one phase worth further examination in calculating single-bolt joints extracted from the bolt array of a built-up propeller blade. Utilizing the rigid body model in the calculation of load distribution in bolt joints without a sealing function causes the required clamping load to be determined by friction grip necessary for transmitting transverse forces. Another possibility would be to consider preventing one-sided opening of the joint instead. However, defining the quantities in that case needs investigating.

The built-up propeller blade design studied in this work has two features whose contribution to load distribution was investigated by modifying the FE model and observing resulting changes in bolt loads. Firstly, the interface between the blade palm and propeller hub is curved, and secondly, there is a step. The 3D model of the built-up propeller blade was modified to be fastened with a flat, planar flange instead of a curved one, and a FE model was constructed of this case too. To test the importance of the step in the geometry, the FE models with both curved and flat flanges were configured in two different ways: both with and without contact between the step surfaces perpendicular to the propeller shaft line. By this configuration, both cases could be studied without modifying the model geometry. The configurations without contact in the mentioned area are approximately equivalent to the case in which the joint interface is a single cylindrical or planar surface.

Results of FEM simulations show that both features, the curved surface and the step in the interface, have a significant effect on the loading of the bolts. Especially the curved shape of the interface makes the bolt loading case totally different from a planar flange, whose bolt joint calculation is instructed in a detailed way in the VDI 2230 standard, and which appears quite simple. At this point it is not clear how the complexities of built-up propeller geometry could be considered reliably in a simple analytical calculation method. To establish one and to develop the calculation tool drawn up in this work into a useful state, several different propeller geometries would need to be examined with the help of FEA.

Although the calculation of bolt load distribution in a better way remains in this work as a phase requiring further research, some conclusions can be made regarding what optimal bolt joints of built-up propeller blades are like. The results of comparing FE models with planar and curved interfaces suggest that a curved one provides more rigidity for the bolt connection, although it is quite possible to shape the propeller hub to have a polygonal outer surface with planar faces. The way of distributing external loading acting on the structure among all bolts, studied in this work, implies that the bolt arrangement should preferably be as close to circular as possible. With slipping of the joined components forbidden, the greatest transverse forces act on the bolts closest to the centroid according to the VDI 2230-2 (2014, 24–25) standard, in which case bolts should lie on a common pitch circle to share transverse loads equally. This holds true on a planar surface but needs further verification in the case of a built-up propeller with a curved joint interface. Considering axial loads, the proportion of tensile force transmitted to each bolt depends on the distance between the load

introduction point and the bolts, and the rigidity of the structure furthermore defines the way the loading is divided (VDI 2230-2: 2014, 92). Ergo, multiple bolts at a similar distance away from the load source are equally loaded. This viewpoint, too, backs the idea of as circular a bolt arrangement as possible.

Besides analytical calculations, the VDI standard instructs calculating bolt joints by utilizing FEM as mentioned in section 4.3. Although that is not the path followed in this thesis, the standard instructions concerning FEM may be helpful in determining the necessary bolt preload, for example, if the FE software utilized does not define it by itself, as was the case in the test calculations of this work.

In addition to a basis for further research within the subject of built-up propeller bolts, the client company of this work is left with an Excel calculation template that can very easily be modified to calculate simpler cases of multi- and single-bolted joints in propulsors. The great majority of all bolt joints have planar interfaces, and many are calculable in the detailed way instructed by the VDI 2230 standard. Constructing the Excel workbook took a significant portion of the time spent working on this thesis, and the finished workbook is its concrete result.

7 Conclusions

The objective of this thesis was to study requirements and methods for designing the bolt joints between the hub and blades of a built-up propeller. The research problem was phrased: how to design the bolt joints of a fixed-pitch built-up ship propeller? A basis for defining the process of designing built-up propeller bolt connections was sought after along with means of checking whether a set of proposed bolts suffice for a propeller design. The research questions leading to an answer to the research problem were how the connection between propeller blades and hub must be designed, what requirements major classification societies have set for bolt joints of built-up propellers and what design methods and processes there are available for use in the maritime industry for designing built-up propellers and their bolt joints.

It was studied in this work what data specific to propeller design is needed and where it can be obtained. Criteria against which the design should be made was found in the rules of classification societies. When it comes to bolt joints, classification requirements reviewed in this work did not differ drastically from each other. For example, the conditions according to which bolts are to be dimensioned for an ice class are identical among the member societies of IACS. Formulae related to bolts appear to be derived from slightly differing starting points, but possible rule differences could affect the design of hydrodynamical propeller blade geometry more.

There are clear strict requirements for ice-classed propellers, which must be designed so that blade loss does not cause massive successive damage, but no such clause was found for non-ice-class, open-water propellers in review of classification rules. With ice blocks in water, there is clearly a greater probability of propeller blades colliding with solid obstacles and thus getting damaged. However, even in iceless, warm conditions it is possible for the propeller to hit ground or rock in shallow waters, for example. If the pyramid strength principle is not followed, the blade is not the first to fail and a collision could damage the propeller hub, shaft and bearings. Compliance with the pyramid strength principle, even if not required, is worth serious consideration. The flip side of the matter is the possibility of using smaller bolts that could be fitted on the blade palm more easily.

This thesis provides the client company a preliminary study to point the way to a workable design process. A Microsoft Excel workbook was constructed for calculating the bolt joints of built-up propellers following the instructions of VDI 2230 standard which takes into account the various aspects related to the loading of bolt joints. Assessing single-bolt joints according to it seems straightforward enough, but the rigid body model utilized in this work proved not to account for the distribution of loading among bolts accurately in the studied case. To calculate single-bolt joints correctly, each of them must be assigned an appropriate portion of the overall load. How to do that on a curved surface is a complicated question. Further developments of the calculation tool before or during a first built-up propeller in-house project should be validated by FEA and comparisons with several different propeller designs and bolt arrangements.

The VDI table for selecting an initial bolt size to try was appended in this work up to M300 from the original M39 in order to ensure an adequate range of choices. The greater the bolt size, the larger tools and greater power is required in installing the bolt joints. The viable maximum size can be defined case by case, but this appended table should not prove to limit making the choice nor need enhancing further.

Temperature-dependence of material properties was consciously omitted in this work but could be later added to the calculation tool. VDI instructs considering the effects of temperature but only lists material properties in room temperature. In the case of propeller design, material properties in colder and warmer conditions would need to be sought. Another matter to investigate is how much exactly seawater affects material properties considered in designing bolt joints.

It would be interesting to compare the minimum bolt diameters suggested by the developed calculation tool with values resulting from formulae of different classification societies' rules and see whether or not the bolt sizes given by the table expanded from the VDI standard systematically satisfy classification requirements. Besides, in a real delivery project, this is a necessary step at least for the part of the particular classification society classifying the vessel to be built anyway. The use of classification societies' calculation formulae requires input from propeller designers with understanding about the relevant quantities from that specialized field.

The calculation tool could rather easily be modified to calculate general bolt arrays utilized in azimuth propulsors with the rigid body model. The fastening bolts of a built-up propeller blade are perhaps in the most complicated environment, but there are numerous bolt joints on flat surfaces and in regular arrangements that would be much simpler cases. The advantage of a calculation tool available for them would be the same as for propeller blade bolts: minimizing bolt size, cost and unnecessary safety factor. Branches of standard instructions different from those noted in this work would possibly need to be followed, but the general structure of the Excel workbook made for the thesis would serve as a solid foundation for modifications for other cases.

The research problem could be answered through alternative approaches to calculating the bolt joints with the help of another standard or theory, so room is left for future studies on the same subject. Literature on propeller design and shipbuilding seems to focus on optimal propeller geometry, and the bolt joints of built-up propellers remain a detail barely looked upon and usually affiliated with CP propellers. Classification rules, while providing requirements for the bolt joints, do not elaborate on the methods by which the joints can be completely defined, although the rules can be used to obtain parts of the solution, as for example in the case of the minimum bolt size.

References

American Bureau of Shipping. 2022a. Propulsion and maneuvering machinery. In: Rules for building and classing marine vessels. Pt. 4. Ch. 3. pp. 193–404. [Online]. [Accessed 2022-05-09]. Available: https://ww2.eagle.org/en/rules-and-resources/rules-and-guides.html#/content/dam/eagle/rules-and-guides/current/other/1_marinevesselrules_2022

American Bureau of Shipping. 2022b. Strengthening for navigation in ice. In: Rules for building and classing marine vessels. Pt. 6. Ch. 1. pp. 1–205. [Online]. [Accessed 2022-05-09]. Available: https://ww2.eagle.org/en/rules-and-resources/rules-and-guides.html#/content/dam/eagle/rules-and-guides/current/other/1_marinevesselrules_2022

Bertram, V. 2012. Practical ship hydrodynamics. 2nd ed. Amsterdam: Butterworth-Heinemann. 391 p. ISBN 978-0-08-097150-6.

Birk, L. 2019. Fundamentals of ship hydrodynamics: fluid mechanics, ship resistance and propulsion. Newark: John Wiley & Sons, Incorporated. 661 p. ISBN 9781118855485.

Bureau Veritas. 2021. Rules for the classification of ships operating in polar waters and icebreakers. NR 527. 50 p. [Online]. [Accessed 2022-04-29]. Available: https://marine-offshore.bureauveritas.com/nr527-rules-classification-ships-operating-polar-waters-and-icebreakers

Bureau Veritas. 2022. Machinery, electricity, automation and fire protection. In: Rules for the classification of steel ships with amendments. NR 467. Pt. C. 587 p. [Online]. [Accessed 2022-04-29]. Available: https://marine-offshore.bureauveritas.com/nr467-rules-classification-steel-ships

Carlton, J. S. 2012. Marine propellers and propulsion. 3rd ed. Amsterdam: Elsevier. 516 p. ISBN 978-0-08-097123-0.

DNV. 2021a. Calculation of marine propellers: class guideline. DNV-CG-0039. 45 p. [Online]. [Accessed 2022-08-03]. Available: https://rules.dnv.com/servicedocuments/dnv/#!/industry/1/Maritime/11/Class%20guidelines%20(CG)

DNV. 2021b. Ice strengthening of propulsion machinery and hull appendages: class guideline. DNV-CG-0041. 94 p. [Online]. [Accessed 2022-06-06]. Available: https://rules.dnv.com/servicedocuments/dnv/#!/industry/1/Maritime/11/Class%20guidelines%20(CG)

DNV. 2021c. Rotating machinery – driven units. In: Rules for classification – ships. Pt. 4. Ch. 5. 87 p. [Online]. [Accessed 2022-04-29]. Available: https://rules.dnv.com/ServiceDocuments/dnv/#!/industry/1/Maritime/1/Rules%20for%20classification:%20Ships%20(RU-SHIP)

DNV. 2022. Cold climate. In: Rules for classification – ships. Pt. 6. Ch. 6. 223 p. [Online]. [Accessed 2022-07-21]. Available: https://rules.dnv.com/ServiceDocuments/dnv/#!/industry/1/Maritime/1/Rules%20for%20classification:%20Ships%20(RU-SHIP)

Doi, M., Nagamoto, K. & Takehira, T. 2013. A study of ship's mooring method with Controllable Pitch Propeller (CPP) by applying generalized minimum variance control. In: 2013 European Control Conference (ECC). pp. 3000–3005. [Online]. [Accessed 2023-10-26]. IEEE. ISBN 978-3-033-03962-9.

Fincantieri. [n.d.]. Controllable and fixed pitch propellers. [Online]. [Accessed 2022-04-25]. Available: https://www.fincantieri.com/globalassets/prodotti-servizi/sistemi-e-componenti/sistemi-e-componenti-navali/pitch-propellers_mp-04-14.pdf

Finnish Transport and Communications Agency Traficom. 2021. Ice class rules and the application thereof. TRAFICOM/68863/03.04.01.00/2021. 65 p. [Online]. [Accessed 2022-05-10]. Available: https://www.traficom.fi/en/transport/maritime/ice-classes-ships

Finnish Transport and Communications Agency Traficom & Swedish Transport Agency. 2019. Guidelines for the application of the 2017 Finnish-Swedish ice class rules. TRAFI/708629/03.04.01.01/2018. Helsinki. 47 p. [Online]. [Accessed 2022-05-10]. Available: https://www.traficom.fi/en/transport/maritime/ice-classes-ships

International Association of Classification Societies. 2007. Machinery requirements for polar class ships. In: Requirements concerning polar class. UR I3 Rev1 Corr1 CLN. 16 p. [Online]. [Accessed 2022-05-10]. Available: https://iacs.org.uk/publications/unified-requirements/ur-i/

Lloyd's Register. 2021. Rules and regulations for the classification of ships. 1808 p. [Online]. [Email address required]. [Accessed 2022-04-29]. Available: https://www.lr.org/en/rules-and-regulations-for-the-classification-of-ships

McGeorge, H. D. 1998. Marine auxiliary machinery. 7th ed. Burlington: Elsevier Science. 514 p. ISBN 0 7506 4398 6.

Rauti, T. 2023. Finite element analysis of a Steerprop built-up propeller bolt joint. [Not public].

Russian Maritime Register of Shipping. 2022. Machinery installations. In: Rules for the classification and construction of sea-going ships. ND no. 2-020101-152-E. Pt. VII. 110 p. [Online]. [Accessed 2022-05-09]. Available: https://lk.rs-class.org/regbook/rules?ln=en

Tupper, E. C. 2013. Introduction to naval architecture. 5th ed. Amsterdam: Elsevier, Butterworth Heinemann. 476 p. ISBN 978-0-08-098237-3.

VDI 2230-1. 2014. Systematic calculation of highly stressed bolted joints. Part 1: Joints with one cylindrical bolt. 2014-12. Berlin: Beuth Verlag. 182 p.

VDI 2230-2. 2014. Systematic calculation of highly stressed bolted joints. Part 2: Multi bolted joints. 2014-12. Berlin: Beuth Verlag. 93 p.

Verein Deutscher Ingenieure. n.d. VDI 2230 Blatt 1 – systematic calculation of highly stressed bolted joints – joints with one cylindrical bolt. [Online]. [Accessed 2022-07-13]. Available: https://www.vdi.de/richtlinien/details/vdi-2230-blatt-1-systematic-calculation-of-highly-stressed-bolted-joints-joints-with-one-cylindrical-bolt